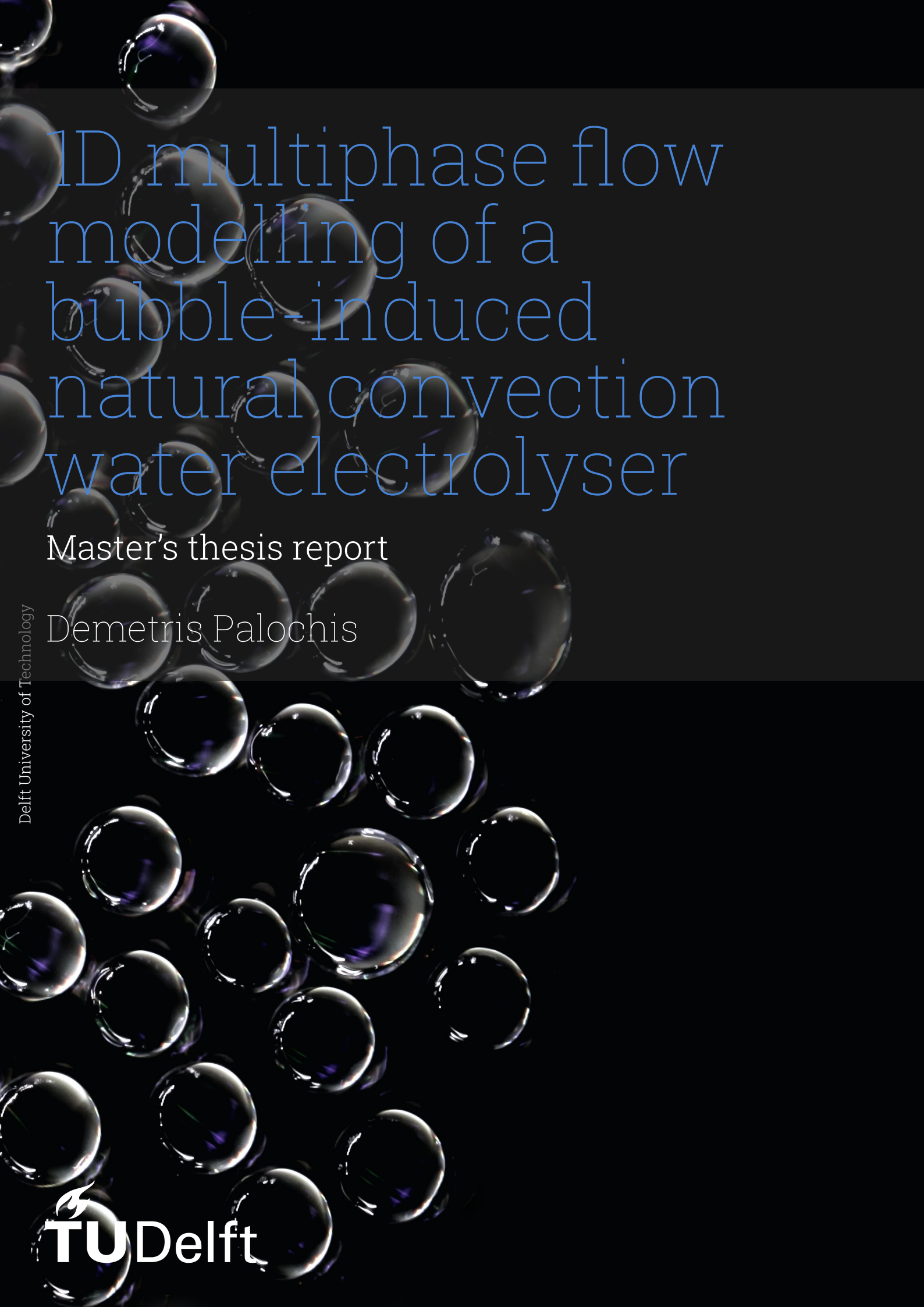

1D multiphase flow modelling of a bubble-induced natural convection water electrolyser

Master's thesis report

Demetris Palochis

Delft University of Technology

TU Delft

1D multiphase flow modelling of a bubble-induced natural convection water electrolyser

Master's thesis report

by

Demetris Palochis

Student Name	Student Number
Demetris Palochis	5376602

Supervisors:	Dr. ir. J.W. Haverkort
	Dr. A. Rahbari
Faculty:	Mechanical, Maritime and Materials Engineering (3mE)
Department:	Energy, Flow and Process Technology
Date:	22nd of January 2023

TU Delft

Abstract

This study focuses on water electrolysis and aims to provide suggestions for the company XINTC Global, for the design of the electrolyser and the accompanying flow network. The most important parameters for this project are the dimensions of the cell, the geometry of the piping network, the electrode gap, the volumetric flow rate and circulation velocity. These parameters influence the performance of the cell. As a result, the production of hydrogen is optimized by fine-tuning these parameters. In addition, the performance in different electrolyser geometries is maximized assuming free circulation of the electrolyte. The geometries differ in the number of cells and the stacking arrangement and they are the single cell, single module and horizontally stacked geometries. The performance indicators are the flow velocity through the electrode gap and the volumetric velocity through the electrode gap, which is a product of the velocity, electrode gap and electrode depth. Furthermore, suggestions on the other dimensions are given, with the aim to maximize the flow rate or velocity. To study the behaviour of the electrolysis system, I developed a Python code that simulates the flow through the electrolysis cell and channel network. This numerical model is compared to an analytical model and experimental data from the literature. Finally, the simulations predicted that the optimum electrode gap width is dependent on the total number of cells. The results with the turbulent flow model, showed that the optimum electrode gaps were 1.85 mm 0.250 mm and 0.250 mm for a single module configuration with 1, 60, and 240 electrolysis cells, respectively. Moreover, the horizontal stacking arrangement of the modules, resulted in larger optimum electrode gaps, for the same number of cells.

Acknowledgments

This project may not have been possible without the guidance of my supervisor. Many thanks to Dr. ir. J.W. Haverkort for his help throughout the project. He has been a great help during my thesis project with his inputs. He was available anytime I reached for advice and he was willing to spend a lot of time on meetings discussing with me problems or the planning for the project.

In addition, I would like to express my gratitude to XINTC Global, which is the electrolyser company I collaborated with for my thesis. Specifically, I would like to thank the lead scientist of XINTC, Dr. Ahmadreza Rahbari, for his help. He was a great support to me with his insights.

Nomenclature

η	Efficiency [-]
μ	Viscosity $[Pa \cdot s]$
ρ	Density $[kg/m^3]$
ε	Gas fraction [-]
E	Energy $[J]$
L	Length $[m]$
r_{b}	Bubble radius $[m]$
u	Velocity of the continuous phase in the x-direction $[m/s]$
U_{g}	Gas flax generation $[m/s]$
W	Superficial velocity, z-axis component $[m/s]$
w	Interstitial velocity, z-axis component $[m/s]$
Δh	Elevation difference $[m]$
δ	Boundary layer thickness $[m]$
$\dot{m}$	Mass flow rate $[kg/s]$
τ	Stress tensor $[Pa]$
A	Surface area $[m^2]$
F	Faraday's constant $[s \cdot A/mol]$
g	Acceleration of gravity $[m/s^2]$
h	Electrode height $[m]$
j	Current density $[A/m^2]$
K_n	Hydraulic friction factor [-], n = 1, 2, 3
l	Electrode gap width $[m]$
M	Molecular weight $[kg/kmol]$
N_{cells}	Number of electrolysis cells per module [-]
N_{el}	Number of electrons invlolved in the reaction [-]
p	Pressure $[Pa]$
Q	Volumetric flow rate $[m^3/s]$
T	Temperature $[K]$
V	Average flow velocity $[m/s]$
w_{el}	Electrode width $[m]$
x	Component on x-axis $[m]$
y	Component on y-axis $[m]$
z	Component on z-axis $[m]$

Contents

1 Introduction

1.1. The role of hydrogen for the energy transition

Climate change and the fossil fuel crisis is challenging the energy sector in the last decade. The transition to a cleaner, more independent source of energy is becoming more and more important. Governments and environmental organizations are making an effort towards cleaner energy sources. The aim is to reduce the emissions of greenhouse gases, like carbon dioxide. Such harmful emissions, occur from energy production with fossil fuels.

A concrete indication of this global effort is the Renewable Energy targets given within the European Union. More specifically, the European Commission has set a target for relying on renewable energy at least by 32%, by 2030 according to the report [1]. The intermittency of renewable energy sources, makes this transition a big challenge.

A solution is to store green energy at times of low demand and high production. Green hydrogen from water electrolysis is a means to long-term energy storage. Combined, with other sectors which require hydrogen, the demand for hydrogen is expected to increase drastically. Figure 1.1, shows how the implementation of hydrogen is expected to reduce carbon dioxide emissions over the next decades, according to ref. [2].

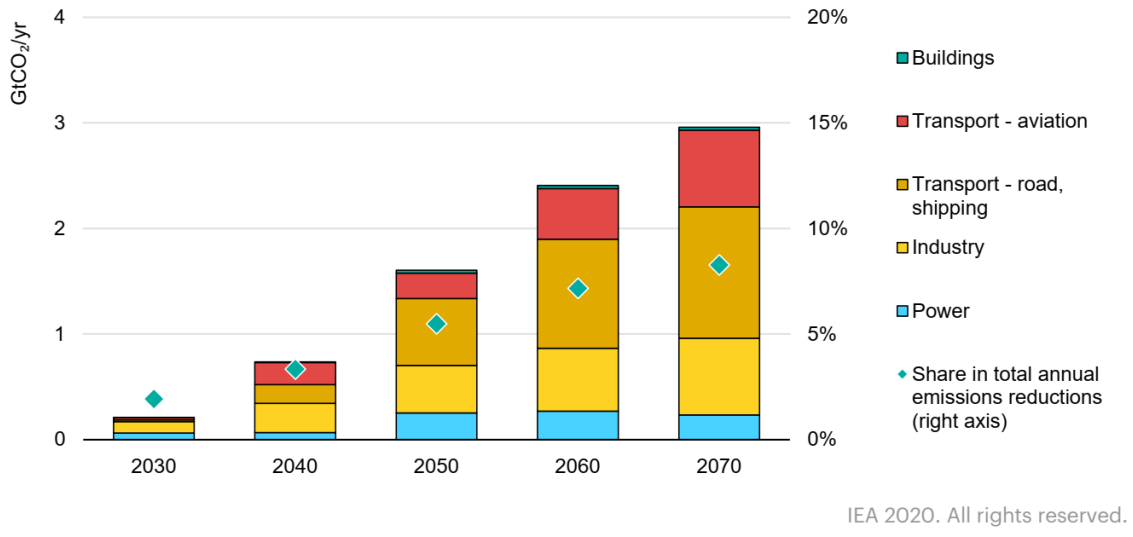

Figure 1.1: Global CO_2 emissions reductions from hydrogen by sector in the Sustainable Development Scenario relative to the Stated Policies Scenario, 2030-70 from ref. [2].

1.2. Hydrogen properties and production techniques

Hydrogen is the first element on the periodic table, and it can be found in abundance on our planet. It is mostly found in the form of water, i.e. hydrogen-oxygen bonds, and organic compounds which can be hydrogen-carbon bonds. It is the lightest element, and it exists in a gaseous phase at normal conditions. To liquefy hydrogen, it requires intense cooling close to absolute zero, pressurizing or both.

Traditionally, hydrogen is produced with fossil-fuel-based processes. The most common are steam reforming with methane and gasification. These methods, emit substantial amounts of carbon dioxide, hence their product is called grey hydrogen. Another method is water electrolysis. It requires electrical power and water and has only hydrogen and oxygen as products. Hydrogen produced from electrolysis, with green electrical power, is called green hydrogen. Green electrical power has zero emissions of greenhouse gases and it comes from renewable energy sources, like wind and solar.

Electrolysis is the electrochemical process of splitting water molecules into hydrogen and oxygen. It is a simple and effective method for the following reasons:

1. Electrical voltage is the driving force of the process, combined with a catalytic material to the reaction.
2. The two gases evolve on different sides of the electrolyser, hydrogen on the cathode and oxygen on the anode. This makes the separation of the gases straightforward. A separator is introduced between the electrodes, to keep the two gases from mixing.
3. No moving parts are required for the electrochemical process.
4. The electrolysis cell can have a simple and repeatable design for scaling up.

As it is mentioned, renewable energy sources are not available on demand, as fossil fuels, and thus green energy needs to be stored. A common way of storing electrical energy is batteries. Although battery technology has made some big advancements over the last few years, it is a short-term solution for energy storage. Batteries are very efficient during charging and discharging, but they tend to lose energy during long periods of time. Batteries also have a short life, they need time to charge and discharge and have a high mass-to-energy ratio. Hydrogen, on the other side, is a better long-term storage.

Hydrogen is an energy-dense compound. A kilogram of hydrogen contains between 33 kWh, which is its Lower Heating Value, and 39.4 kWh, which is its Higher Heating Value, [3]. Figure 1.2 illustrates the differences between Hydrogen and common fuel types. Hydrogen has a high energy-to-weight ratio compared to other types of fuel. In contrast, hydrogen has a lower energy-to-volume ratio since it is found in a gaseous form at normal conditions.

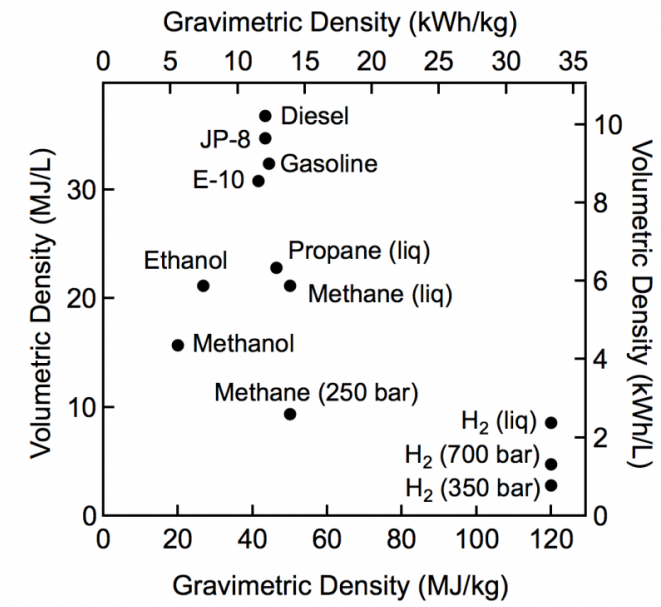

Figure 1.2: The volumetric energy density as a function of the gravimetric energy density of common fuels from ref. [4].

1.3. Water electrolysis

Different types of water electrolysis cells exist. The cells are identified either as alkaline or acidic. An alkaline environment in the cell corresponds to a pH value higher than seven, whereas an acidic one corresponds to a pH value lower than seven. As it was explained earlier, water is the reactant of the electrochemical process. To achieve either environment, alkaline or acidic, water-based solutions are used. For example, in an alkaline cell, a KOH-water solution is used. This mixture is called the electrolyte.

During electrolysis, cell voltage is applied between the anode and the cathode to produce hydrogen and oxygen. For an alkaline cell, hydroxide molecules HO^-, take the role of charge carriers and transport by diffusion and convection from the cathode to the anode. The partial reactions, and a typical cell configuration, are illustrated with figure 1.3. a, from ref. [5].

Similarly, in the acidic cell, there is an abundance of hydrogen ions H^+ which function as the energy carriers and transport from the anode to the cathode side. In figure 1.3. b, the partial reactions, and a typical cell configuration for acidic electrolysis is illustrated.

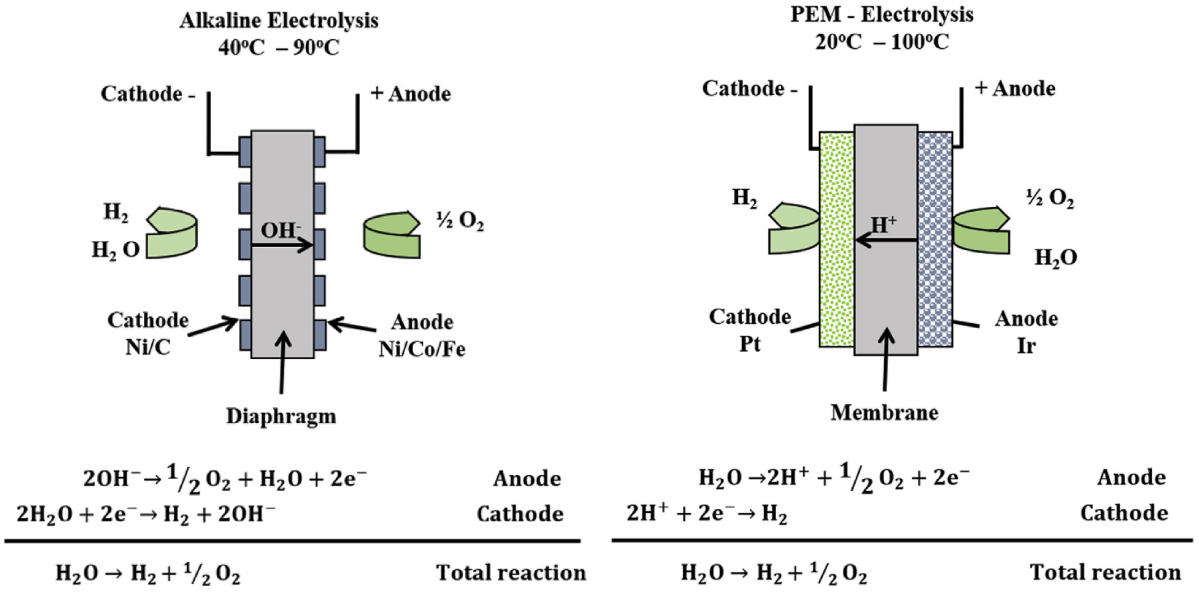

(a) Typical alkaline electrolysis cell from ref. [5]

(b) Typical acidic electrolysis cell from ref. [5]

Figure 1.3: Comparison between alkaline and acidic (PEM) electrolysis.

1.4. Current density

Current density j is related to the rate of hydrogen production. It has units of Amperes per square meter, as it represents the electrical current through the cell. The hydrogen production is given below by Faraday's law with equation (1.1).

$$\dot{m} = \frac{M}{N_{\text{el}} F} jA \tag{1.1}$$

where M is the molecular weight of hydrogen, N_{el} is the number of electrons involved in the reaction of electrolysis, F is the Faraday constant, j is the current density and A is the geometric surface area of the electrodes.

1.5. Electrode gap

An important design parameter for the electrolyser is the distance between the electrodes, which is called inter-electrode gap. Furthermore, the distance between the electrode and the separator is considered for this study and it will be referred to as electrode gap. It is preferable since it is used for the calculation of the pressure drop.

Figure 1.4 from ref. [6], indicates the inter-electrode distance on a traditional electrolysis cell. For the study of the flow, it is important to use the gap between solid surfaces. Therefore, the distance between

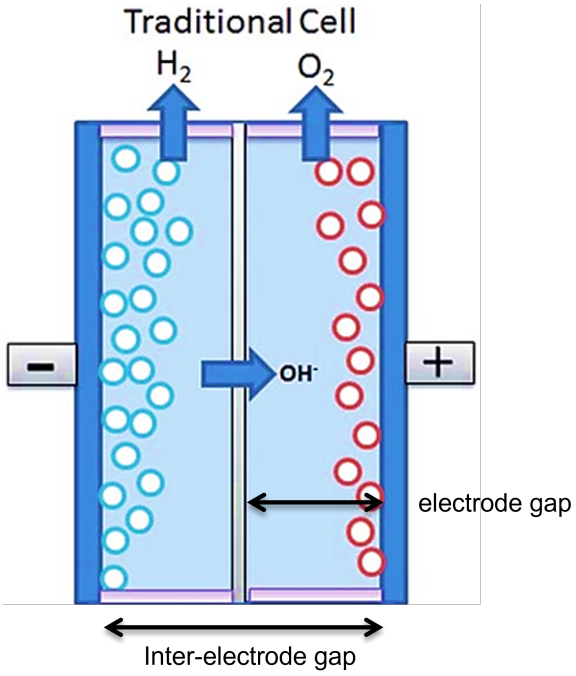

Figure 1.4: Illustration of the inter-electrode gap and electrode gap of a traditional alkaline cell from ref. [6]. The blue plates on the left and right side are the electrodes.

the cathode and the separator is considered, which is equal to the distance between the anode and the separator. Then this distance equals half of the inter-electrode distance, minus half of the separator thickness.

Generally, the over-potential due to the thickness of electrolytic solution between the electrodes increases with the electrode gap width. To decrease this resistance, the electrode gap can be decreased. When the gap becomes zero, the electrodes are pressed onto the separator, a cell configuration known as a zero-gap configuration. A zero-gap cell and cells with smaller gaps, require a perforated electrode, so gas bubbles can escape to the other side of the electrodes. In the zero-gap alkaline cell example, in figure 1.5 from ref. [7], the electrodes are made of a woven material and they are pressed onto the diaphragm. For this type of cell, the over-potential due to the inter-electrode distance is at a minimum, but another over-potential appears. The gas bubbles have limited space to move and as a result, they tend to stick to the electrode surface and accumulate. Consequently, there is less effective electrode area for gas evolution and the efficiency of the cell drops.

The zero-gap configuration is investigated by ref. [8]. In this article, the effect of gas bubbles is studied experimentally. The researchers concluded that the bubbles block a significant amount of the electrode surface. As a result, the surface of the electrode towards the separator was entirely blocked. They proposed a small gap between the separator and the electrodes. Despite the increase in the electrolyte over-potential, this nearly zero-gap configuration is found to be beneficial by allowing some room for the bubbles to escape.

1.6. Electrode height and gas cross-over

It is the dimension of the electrode in the direction of the flow. The electrode height has an impact on the gas fraction since the electrode surface is increasing as the height is increasing, with constant cross-section area, safety issues arise.

As the gas fraction increases, the gas that escapes through the separator to the other side of the cell increases. This phenomenon is called gas cross-over, and it becomes an important limitation. It is defined as the amount of hydrogen on the oxygen side or anode side. A maximum gas cross-over of about 4% is strictly imposed for safety reasons because above this percentage there is a risk of explosion. This performance aspect for the electrolyser is out of scope, and it will not be investigated during this study.

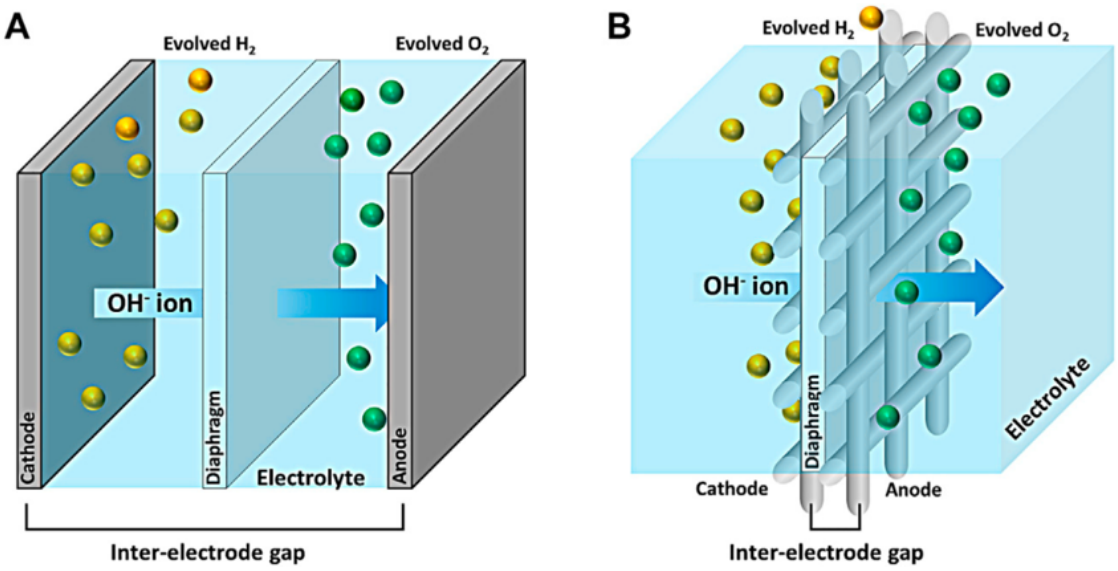

Figure 1.5: Comparison of a traditional and a zero-gap cell from ref. [7]. On the left is the traditional cell, with solid plate electrodes. On the right is the zero-gap cell with woven mesh electrodes.

1.7. Gas volume fraction

When gas is evolving on the electrodes, hydrogen on the cathode and oxygen on the anodes, gas bubbles are formed. The bubbles occupy the volume in the electrolyte flow. This change in volume is important for estimating the flow velocity, as it increases by increasing the total volume of the mixture. Thus, gas is measured in volume. More specifically, it is measured as the gas volume relative to liquid volume. This relation is called volume fraction.

The volume fraction is estimated by dividing the local gas volume by the liquid volume. The gas volume value is given by Faraday's law of electrolysis, as it is found in the book [9].

1.8. Recirculation velocity

It is the average velocity of the gas-liquid mixture through the electrode gap. The flow is necessary for removing the gas bubbles from the electrode gap and maintaining a low gas volume fraction. The higher the flow velocity, the less gas is accumulated in the cell.

This flow induces heat transfer and mass transfer because the liquid carries the thermal energy produced during electrolysis, which is usually discarded from the system with heat exchangers outside the electrolysis cell. The flow is also important for removing the produced gas and replacing the gas-liquid mixture with pure electrolyte.

1.9. Natural convection

The electrolyte flow can occur either from forced flow or natural convection flow. Forced flow is induced by means of an external pump, which operates on an external power supply. This additional power can be saved by opting for a natural convection flow. Natural convection is created due to gravity with buoyancy effect on gas bubbles and electrolyte liquid. As shown in figure 1.6, the mixture density in the riser column decreases due to gas bubbles. Then, the force of gravity combined with the difference in density creates a pressure difference across the electrolysis cell and the separator tank, thus flow occurs. This effect can be amplified by adjusting the dimensions of the cell and the surrounding channels.

1.10. Motivation for studying natural convection electrolyser

An electrolyser cell requires flow parallel to the electrodes' surface to extract gas bubbles from the electrode gap. As it was explained earlier, bubbles introduce a resistance to the current since they occupy the volume of the conductive medium, which is the electrolyte liquid mixture. Therefore, it is

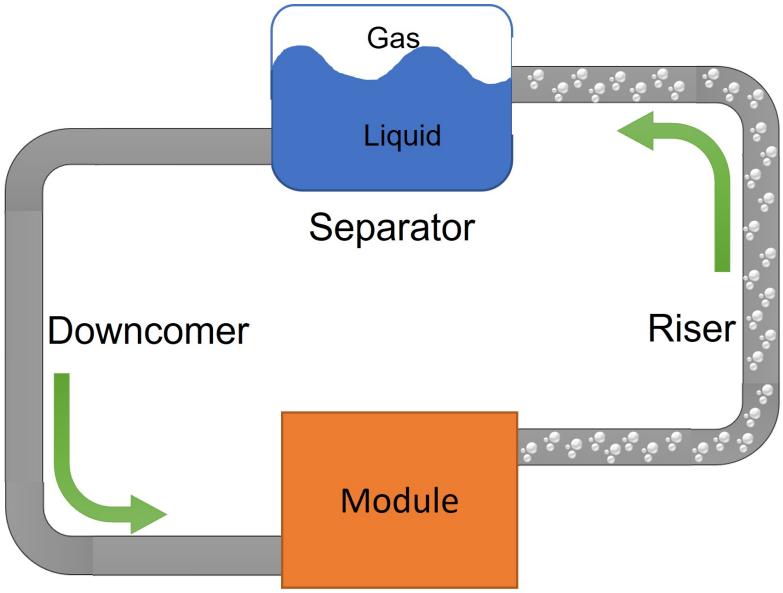

Figure 1.6: Water electrolyser, with a flow induced by natural convection.

essential to have sufficient flow through the cell. Flow depends upon a driving force, which is usually a pump. Although the pump gives control of the flow velocity, it consumes energy.

Another solution to keep the electrolyte flowing, is to take advantage of the buoyancy force on the gas bubbles. This force occurs from the acceleration of gravity and is called natural convection. It requires no additional power; thus it can be an effective solution of minimizing the overall energy efficiency of the electrolysis cell. As a result, the requirements for an electrolysis cell with natural convection flow, includes only the power for the electrochemical reaction.

Consequently, the electrolysis system becomes less complex in terms of components and devices. On the other hand, the system geometry has now a significant effect on flow as well as on efficiency. Therefore, the goal is to design the geometry such as the buoyancy force is large enough to overcome the friction forces and recirculate the electrolyte liquid. The current study aims to prepare a model, which acts as a prediction tool for flow velocity. Then this tool should facilitate the designing process by giving suggestions for the geometry.

1.11. Network of channels

As it is explained above, an electrolyser operating under natural convection conditions, induced by gas bubbles, can be optimized for maximum circulation velocity or volumetric flow rate. The optimization will occur on the dimensions of the cell, on the current density and on the dimensions of the channels. There are multiple pathways for the electrolyte to enter the cell as well as for the gas-liquid mixture to exit the cell. There are also distributors that divide the flow to multiple cells, as well as collectors which combine the outlets of the cells. Furthermore, pure electrolyte is transported to the cells through a vertical column called the downcomer and the mixture is removed through another column called the riser. The geometry of such a network is illustrated with figure 1.6, where one module with electrolysis cells is included. All of these channels and connections create the network of channels which was mentioned earlier. The most important dimensions of this network will be optimized during this project for maximum circulation velocity. The dimensions are:

- Electrode gap width
- Height of the electrode
- Downcomer diameter
- Riser diameter

2 Theory

2.1. Over-potential and cell efficiency

An important aspect for the financial feasibility of an electrolyser is efficiency. One type of efficiency for electrolysis cells is voltage efficiency, which is the ratio of thermoneutral potential and cell potential. Thermoneutral potential is defined as the voltage at which electrolysis occurs without any heat supply or heat sink (adiabatic conditions). This means that all thermal energy required for the total reaction is provided by electric current. For equilibrium conditions, (25 °C, 1 bar), thermoneutral potential is equal to 1.48 V. Voltage efficiency is given below with equation 2.1 as it is found from [10].

$$\eta_U = \frac{U_{\text{thermoneutral}}}{U_{\text{cell}}} \tag{2.1}$$

where η_U is the voltage efficiency, and it is a percentage, $U_{\text{thermoneutral}}$ is the thermoneutral potential and U_{cell} is the voltage applied across the electrolysis cell. For example, a cell with 80% voltage efficiency, is operating at 1.85 Volts of cell voltage.

Cell voltage is defined by the over-potential in the cell. Over-potential is the additional voltage provided for electrolysis, to account for losses. There exist three sources of over-potential:

1. Activation over-potential (η_{act}): It is a loss caused by the activation energy required for electrolysis. It is calculated separately for the anode and cathode. The value of the over-potential depends on the catalytic material used for the electrodes and the temperature at which the reaction takes place. Better materials, and higher temperatures, can reduce the activation over-potential.
2. Ohmic over-potential (η_{ohm}): It is the superposition of the electric resistances in the cell, including the resistance from the electrolyte. Higher electrolyte conductivity, lower current densities, higher temperature, better materials and the geometry of the cell can reduce this over-potential.
3. Concentration or diffusion over-potential (η_{con}): It is the loss due to mass transfer restrictions of hydroxide immediately adjacent to the anode surface. At low current densities, diffusion is fast enough and marginal concentration over-potential is observed. At high current densities, the diffusion is not quick enough to keep up with the depletion of hydroxide on the anode surface, as it is studied by [8].

The minimum cell voltage, also called reversible voltage (U_{rev}) is the minimum voltage at which electrolysis is happening. At this voltage, an external heat source is required. It is equal to 1.23 V at 25 °C and 1 bar. The cell voltage is given as the summation of the minimum cell voltage and the over-potentials. Cell voltage is presented below with equation 2.2.

$$U_{\text{cell}} = U_{\text{rev}} + \eta_{\text{act}} + \eta_{\text{ohm}} + \eta_{\text{con}} \tag{2.2}$$

2.2. Effect of bubbles on cell voltage and efficiency

The efficiency of an electrolysis cell is a function of numerous parameters. Amongst others, the accumulation of gas bubbles in the electrode gap has a negative impact on cell voltage which is

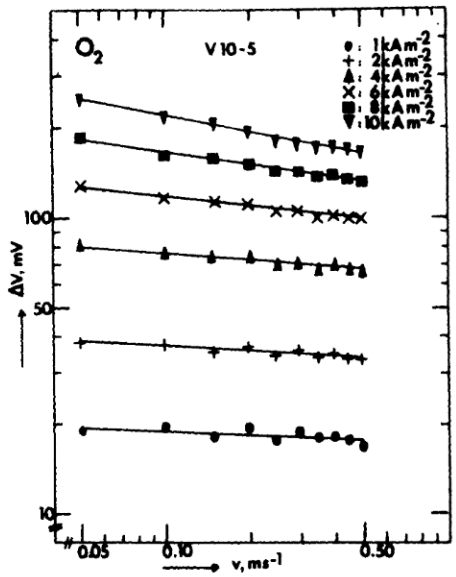

Figure 2.1: Potential drop ΔV across one electrolysis cell as a function of flow velocity, from [11].

synonymous with the electrical efficiency of the cell. As gas bubbles evolve in the electrode gap, part of the electrolyte volume is displaced by lower conductivity gases, either oxygen or hydrogen. As a result, the resistance of the electrolyte increases and the required voltage across the cell is increased to achieve the same current density.

Less gas is accumulated as the flow velocity increases and voltage decreases. This is nicely illustrated by [11] with figure 2.1. They suggest that to maintain a current density, the potential difference across the electrodes decreases as the flow velocity increases. A similar phenomenon was observed by [12], where the current density increases as the mass flux through the electrode gap increases for constant voltage across the electrodes. The reason is the faster removal of gas bubbles, which then translates to lower gas fraction values in the electrode gap and lower ohmic losses.

At the same time, the bubbles are randomly dispersed in the electrolyte, the ions are forced to take a longer path around them to move from the cathode to the anode. This measure is called tortuosity. When the shortest path is a straight line, tortuosity is equal to one and when the path is longer, tortuosity is greater than one. Then, electrolyte resistance increases even more with tortuosity.

Consequently, for this project, the circulation velocity is the key performance indicator for the optimization of the electrolyser system. This means that the aim is to maximize the velocity because higher velocities showed less required voltages, thus better overall efficiency of the cell. At the same time, higher volumetric flow rates results in lower gas fractions.

On the other hand, volumetric flow rate is a product of flow velocity, electrode gap width and electrode depth. Thus, for the case of very narrow electrode gaps, high gas fractions can occur for high flow velocities in the gap. Since the gap width is small, a high flow velocity can occur but the volumetric flow rate is still not sufficient to quickly remove the gas. As a result, the volumetric flow rate is investigated for this study, especially for the narrow gap widths.

2.3. Predicting circulation velocity

In a water electrolysis cell or other kind of electrolysis, a parameter that increases the ohmic resistance is the gas fraction of the mixture. To overcome the accumulation of bubbles, the flow of the electrolyte should be sufficient, so the gas is removed effectively.

Researchers have used the value of circulation velocity as a performance indicator, especially for natural convection cells. For example, [13], has predicted the velocity profile in a fluorine electrolysis cell via a numerical model. They used skirts, which are the two solid surfaces at the inlet that guide the flow towards the electrode. The skirts augmented the effect of flow in the cell to improve the separation of gases.

Similarly, in [14] they have estimated the circulation velocity in an airlift reactor. For this publication, they used an energy balance approach, and they managed to develop a model based on many parameters and consider various sources of energy loss. In comparison, the final product of these publications was a numerical model predicting the velocity. Each model has a variety of input parameters, which can be adjusted quickly so the geometry of the cell or the operating conditions are approached differently. Then, it is obvious that valuable conclusions can be obtained with experimentation on the models, during the design process of a cell. Therefore, they are considered important tools for optimizing the final design.

This study aims to develop such a tool for a water electrolysis cell. Specifically, an alkaline electrolyser is assumed under natural convection conditions. Due to the absence of an external driving force for the flow, there is no means of actively controlling the velocity. The prediction of the circulation velocity is important for tuning the geometry, to achieve high efficiency.

2.4. Modelling

In this section, the modelling of the cell is discussed, which requires a combination of the discussed topics.

Modelling a water electrolysis cell has the purpose of describing its function with mathematical formulas. Then calculations are executed to obtain a better understanding of the cell. Such an approach had been taken by a few researchers with different outcomes.

The work in [15], is an example where the researchers modelled the flow inside an electrolysis cell. They focused on a free-circulating cell, and they managed to show how varying the dimensions of the cell can positively affect the volumetric flow rate. The researchers from [14], have modelled the flow in an airlift reactor, which is a different device. It is a closed loop channel, where the liquid and gas are mixed via the injection of the gas on the bottom of the riser column. Nevertheless, the aim was the same, to predict the circulation velocity of the liquid in the riser. More research on modelling is found in the work of [16]. In this case, a more complex phenomenon is investigated, the backflow which appears on the top part of the riser, as it was explained in a previous section. The model developed by the researchers correlates the ratio of gas flow rate over liquid flow rate to the ratio of Froude over Reynolds dimensionless numbers.

Modelling an electrolysis cell can provide an understanding of the flow pattern, as it was shown in the examples above. A model can also predict the resistance of the electrolyte, which is the case for [17]. This article is focused on the over-potential due to the electrolyte under various conditions. A two-phase numerical model is developed and compared to an analytical model. It considers different operating conditions such as pressure, current density as well as the electrolyte width which is a geometric parameter.

Finally, modelling of the flow in an electrolysis cell was previously coupled with simulations. An example of such a work is [18]. The aim of the researchers was to initially model and then investigate with numerical simulations a two-phase electrolysis cell. They developed an electrical model which describes the gas evolution relative to the applied cell voltage. Besides, they described the hydrodynamics of the cell by modelling the flow and executing simulations with computational fluid dynamics software. In figure 2.2, results from the simulation are presented. The figure shows how the flow develops across the electrode. At the bottom, a Poiseuille flow profile is defined, which has the maximum velocity in the centre. We can observe that the simulation predicted a velocity profile where the maximum is closer to the left side, where the electrode is located.

2.5. Maximum gas volume fraction

The volume fraction of phase A in a two-phase mixture, with phases A and B, has values between zero and unity. This means that the mixture can consist 100% out of phase B or 100% out of phase A or can consist of a combination of the two phases in any other percentage in-between.

In the case of electrolyte and gas bubbles mixture, this is not the case. Assuming that gas bubbles are spherical and have the same diameter, there is a geometrical limitation to the volume fraction. The highest volume fraction can be achieved with a hexagonal close-packing or square close-packing arrangement of spheres. These dense arrangements assume that the spheres are perfect and equal in diameter. The volume fraction of spheres occupying space is equal to $\frac{\pi}{3\sqrt{2}} \approx 0.74048$ according to [19].

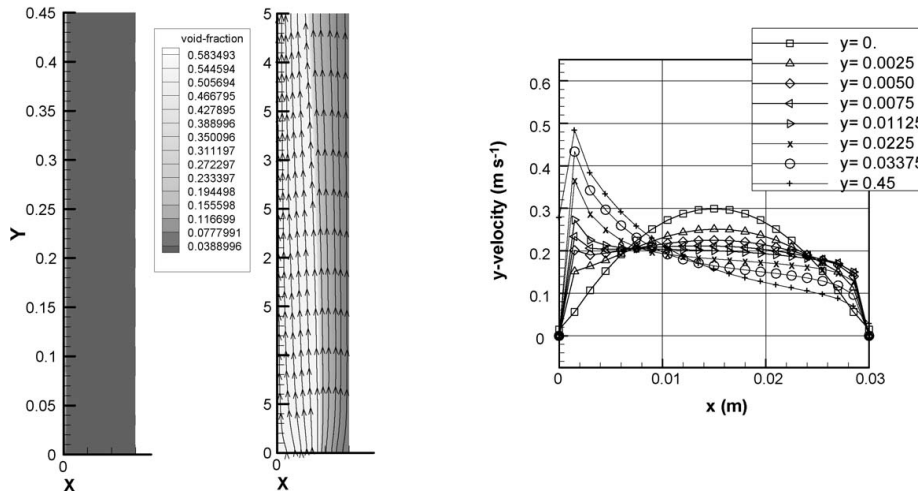

Figure 2.2: CFD simulation results from [18]. On the left, the flow paths are presented. On the right, the velocity profiles are given at various locations in the domain

In addition, repelling forces between the gas bubbles are responsible for keeping a distance between them. Thus, the volume fraction of gas bubbles occupying space in the electrolyte is lower than 0.74048.

2.6. Viscosity as a function of gas volume fraction

The viscosity of pure water can be altered by increasing or decreasing the temperature. For a water-based electrolyte, the amount of dissolved substance, which is usually KOH for alkaline electrolysers, the concentration can also affect the viscosity, at a constant temperature. Furthermore, when hydrogen and oxygen bubbles are evolving in the electrolyte, viscosity changes, because particles in a two-phase mixture, introduce additional friction which translates to viscosity. It is important to understand the effect of gas fraction, to predict how viscosity is changing in the electrode gap because of gas evolution.

The goal is to maintain a gas fraction which results in a relatively low viscosity and as a result in small losses due to viscous forces in the flow. In a natural recirculation electrolyser, it is important to minimize losses, since there is no external pumping power to counterbalance the resistance.

To approach the effect of gas volume fraction on mixture viscosity, the model given below is used. Equation (2.3) gives mixture viscosity as a function of the gas fraction. Figure 2.3, illustrates this relation, which suggests that, as the gas fraction increases, mixture viscosity increases. For gas fractions below 0.8, a small increase in viscosity is observed and for gas fractions close to 1, a steep increase is shown. Though in practice, the gas fraction has a maximum value below 0.74048, which is the geometrical maximum value.

This correlation is studied experimentally by [20] and illustrated on a plot of mixture viscosity as a function of gas fraction with figure 2.4. The experimental results suggest an increase in viscosity as well, with a slightly different trend.

$$\mu_m = \frac{\mu_l}{1-\varepsilon} \tag{2.3}$$

At the same time, it is important to note that there is a maximum value for gas volume fraction, which is given by the geometric arrangement of gas bubbles and the interaction between the bubbles in the alkaline environment. This maximum value for the gas volume fraction will be discussed later in a separate section.

2.7. Density as a function of gas volume fraction

Similarly to mixture viscosity, mixture density needs to be adjusted based on the amount of gas evolved in the electrolyte. Gas bubbles occupy space in the fluid, thus the average density decreases since the density of hydrogen and oxygen are much lower than the density of the electrolyte. Therefore, the mixture viscosity is calculated as the volume-weighted average of the viscosities of the two phases in the flow. Equation (2.4) is suggested by [21] and gives a linear relation of mixture viscosity and the gas

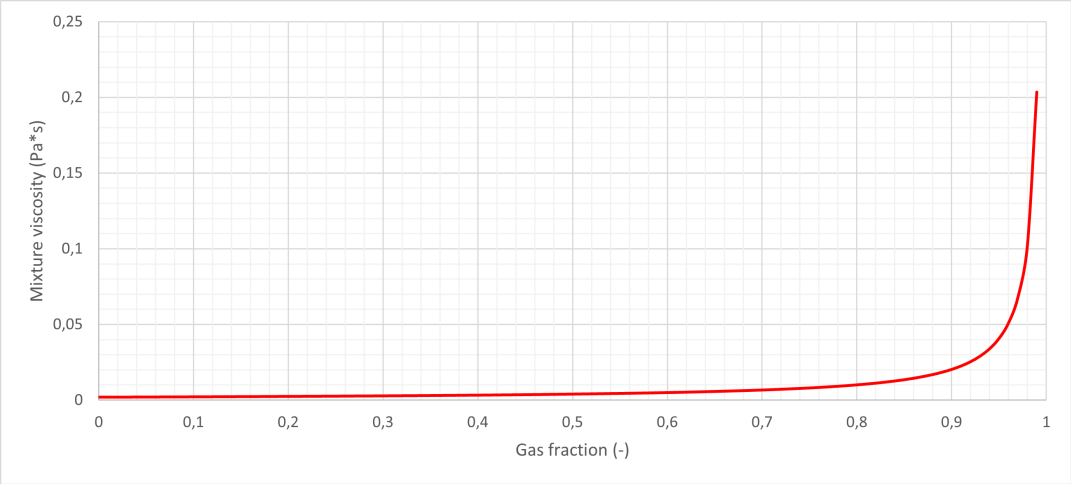

Figure 2.3: Mixture viscosity as a function of the gas fraction.

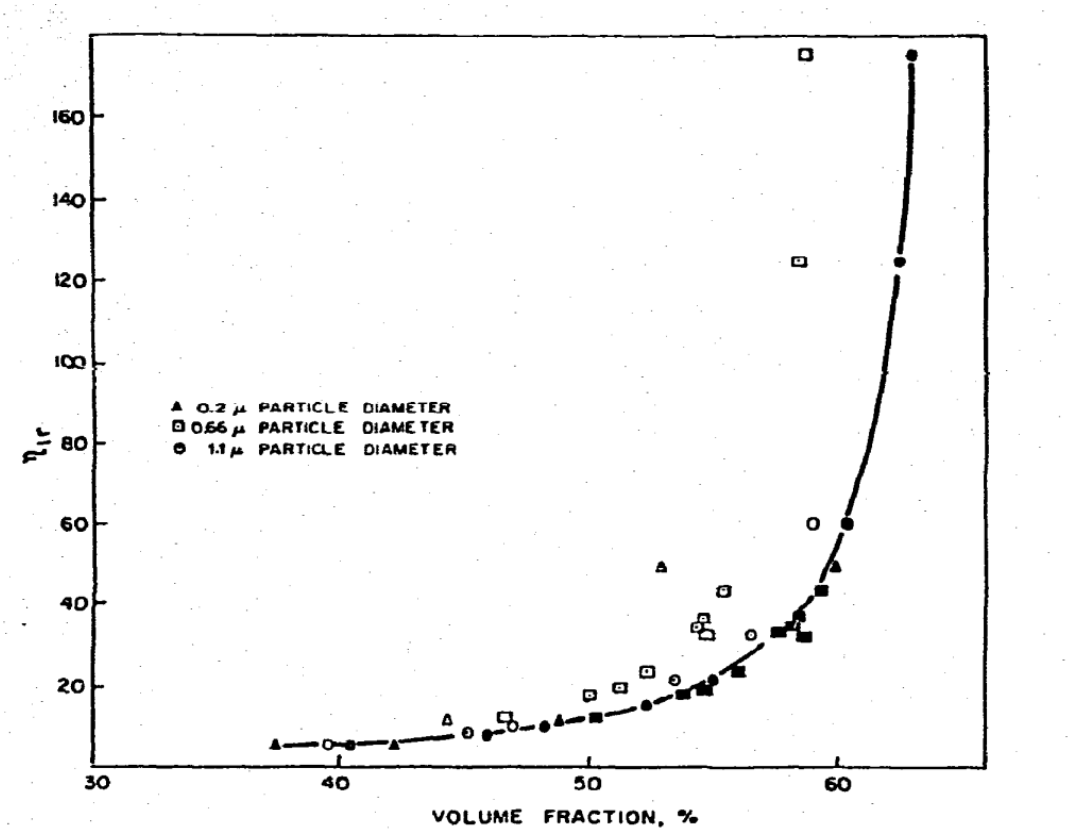

Figure 2.4: Relation of mixture viscosity to particle volume fraction, from [20]

fraction, which is illustrated with figure 2.5.

$$\rho_m = \rho_l \varepsilon_l + \rho_g \varepsilon_g \tag{2.4}$$

where ρ_m is the mixture density, ρ_l is the density of the liquid phase, ε_l is the liquid volume fraction, ρ_g is the density of the gaseous phase and ε_g is the gas volume fraction. By substituting the liquid volume fraction ε_l with $1 - \varepsilon_g$, a function of mixture density as a function of gas volume fraction is obtained, shown with equation (2.5).

$$\rho_m = \rho_l(1 - \varepsilon_g) + \rho_g \varepsilon_g \tag{2.5}$$

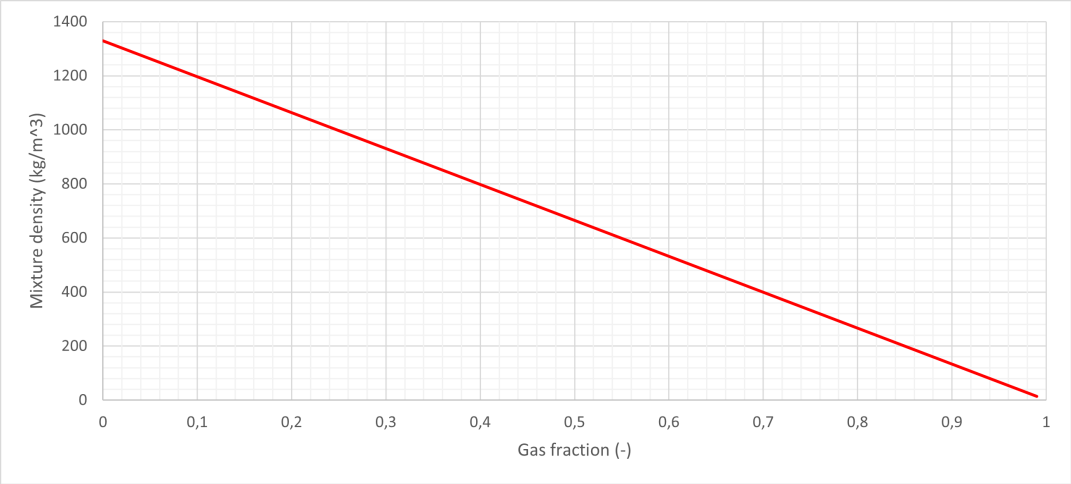

Figure 2.5: Mixture density as a function of the gas fraction.

2.8. Velocity

In multiphase flow theory, velocity can be measured in two ways. Therefore, two definitions of velocity exist. The first one is interstitial velocity. It describes the velocity of the electrolyte fluid travelling around bubbles in a gas-liquid mixture. It is given by equation (2.6).

$$w = \frac{w_s + W}{1 - \varepsilon/\varepsilon_m} \tag{2.6}$$

where w_s is the slip velocity, W is the superficial velocity and ε_m is the maximum gas volume fraction.

Assuming no slip velocity $w_s = 0$ and a maximum gas fraction of 1 $\varepsilon_m = 1$, the interstitial velocity is then given by equation (2.7).

$$w = \frac{W}{1 - \varepsilon} \tag{2.7}$$

The interstitial velocity increases as the gas volume fraction increases, since the same electrolyte has to move through a smaller cross-section area. Moreover, as the slip velocity and the superficial velocity increase, interstitial velocity increases. The second definition is superficial velocity. It refers to the volumetric flow rate of the fluid, divided by the cross-section area. When we have a flow of a two-phase mixture, the superficial velocity is calculated with the volumetric flow rate of the phase of interest, over the total cross-section area that the mixture is flowing through. When the flow consists of a single phase, then the superficial velocity becomes equal to the interstitial velocity of the fluid.

$$W = \frac{Q}{A} \tag{2.8}$$

where W is the superficial velocity, Q is the volumetric flow rate and A is the cross-section area.

For the current study, a two-phase flow is considered, where the mixture consists of a liquid (e.g. water or electrolyte solution) and a gaseous phase in the form of small bubbles. As it was explained earlier, the mixture quality is described with gas volume fraction, which is the ratio of the gaseous over the liquid phase, in volumes.

2.9. K-value and Friction factor

For the modelling of the flow components and flow channels, the calculation of K-values was necessary. K-value is a friction factor that is required for the calculation of hydrodynamic pressure loss. This difference in pressure is found in internal flows due to the friction between the flowing liquid and the solid walls. To arrive at the K-value of a flow channel first we need to calculate the Reynolds number of the pipe section with equation (2.9).

$$\mathrm{Re} = \frac{\rho W L_{\mathrm{char}}}{\mu} = \frac{inertia\ forces}{viscous\ forces} \tag{2.9}$$

Then, we calculate the Darcy friction factor which is calculated with equation (2.10) for laminar flow and with equation (2.11) for turbulent flow.

$$f_D = 4\sqrt{3.8ln\left(\frac{10}{Re + 0.2 * \epsilon/D}\right)} \tag{2.10}$$

where ϵ is the roughness of the pipe material, which for PVC piping is $\epsilon = 0.002\ mm$.

$$f_D = \frac{16}{Re} \tag{2.11}$$

The K-value for a straight pipe section is calculated with equation (2.12).

$$K = f_D \frac{L}{D} \tag{2.12}$$

Equation (2.13) is then used for calculating pressure loss value.

$$\Delta p_{\text{loss}} = K\frac{1}{2}\rho W^2 \tag{2.13}$$

Furthermore, in pipeline modelling, standard values for K-values are found from tables. For example, for a bend and a tee-joint, the K-values are 0.75 and 1.0, respectively. Finally, the summation of the pipe sections in series gives the pressure drop value for the pipeline.

2.10. Friction body force

The current study aims to predict the flow velocity inside the electrolysing cells. The most important factors that affect the velocity are the driving force which is the hydrostatic pressure difference and the resisting forces. The two driving and resisting forces oppose each other, arriving at a balance in which the electrolyser operates at a steady state with a constant flow velocity through the cells. The resisting forces consist of various terms, amongst which is the friction forces or viscous forces. Friction forces dominate the resisting forces because of the relatively high viscosity of the fluid mixture and low velocities. In this section, the friction forces are explained.

In order to estimate the recirculation velocity of the electrolyte, the pressure drop across the cell is required. Consequently, a relation between the pressure drop and the operating conditions and fluid properties is considered. Such a relation is found in Hagen-Poiseuille law, which applies for laminar flow regimes. The equation in its general form is written as:

$$\Delta p = \frac{8\pi\mu_m LQ}{A^2} \tag{2.14}$$

where Δp is the pressure drop across the pipe section of interest, ρ is the density of the liquid flowing through the pipe section and V is the average flow velocity.

For turbulent flow regimes, Darcy-Weisbach equation is widely used and it is given below in equation (2.15).

$$\Delta p = f_D \frac{\rho v^2}{2D_H} \tag{2.15}$$

Both equations correlate the pressure drop with the fluid density and the fluid velocity. Consequently, solving the equation for velocity, gives the velocity for a known pressure drop.

To arrive at an equation, which provides the friction forces due to the flow inside the pipes, a series of equation manipulations occurred. First, we begin with the definition of the Hagen-Poiseuille law, given in equation (2.14). Then, the interstitial velocity is substituted with the superficial velocity, which is given as equation (2.7).

2.11. Numerical model

The current section has the purpose of going through the steps taken during the modelling of the electrolyser system. The system is explained with a schematic, as well as a set of equations that explain the physics involved. The derivation is based on the guidelines given by ref. [22].

The fundamental equations are momentum conservation and mass conservation, which can be found in appendix A.

From [22], the momentum conservation for 2D flow is given with equation (2.16). In this form, the equation describes the momentum on a 2D plane, on x- and z- axes. On the left side are the inertial terms for x and z and on the right side are the pressure, viscous and gravity terms.

$$\frac{\partial \rho(1-\varepsilon)w^2}{\partial z} + \frac{\partial \rho(1-\varepsilon)uw}{\partial x} = -\frac{dP}{dz} + \frac{\partial}{\partial x}\left(\mu_{\text{eff}}\frac{\partial w}{\partial x}\right) + \rho\varepsilon g \tag{2.16}$$

with the pressure

$$P = p + \rho g z \tag{2.17}$$

where ρ is the liquid density, ε is the gas fraction, w and u are the velocities along the $z-$ and $x-$ axes respectively, μ_{eff} is the effective viscosity of the mixture p is the pressure and g is the acceleration of gravity.

Additionally, from [22], the mass balances for the electrolyte fluid and for gaseous hydrogen in the system are given in equations (2.18) and (2.19).

$$\frac{d\left(\rho_g \varepsilon(w + w_s)\right)}{dz} = \frac{jM}{nFl} \tag{2.18}$$

where ρ_g is the hydrogen density, w is the electrolyte interstitial velocity and w_s is the slip velocity.

$$\frac{d\rho(1-\varepsilon)w}{dz} = 0 \tag{2.19}$$

Then, we assume the properties of the mixture and the flow velocity are constant across x and they change across the flow direction which is parallel with the z axis. The axes are illustrated in figure 2.6.

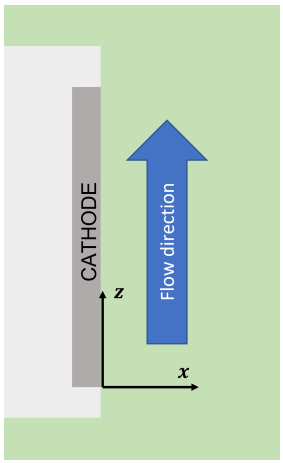

Figure 2.6: The schematic of the cathode side of one cell. The green domain is the flow channel and its width represents the electrode gap. The boundary on the right side of the green domain is where the separator surface is located.

The next step is to obtain a 1D equation. By averaging (2.16) across the $x-$axis and assuming no flow on the horizontal direction $u = 0$, we arrive at equation (2.20).

$$\frac{\partial\langle\rho(1-\varepsilon)w^2\rangle}{\partial z} = -\frac{d\langle P\rangle}{dz} + \frac{\tau_w}{l} + \langle\rho\varepsilon\rangle g \tag{2.20}$$

where, by definition the shear stress is $\tau_w = \left(\mu_{\text{eff}}\frac{\partial w}{\partial x}\right)_{x=0}$ at the wall surface.

Finally, equation (2.20) is averaged across the electrode height h by $\frac{1}{h}\int_0^h dz$, to arrive at a discrete form. Then, equation (2.21) is obtained, as it is suggested in ref. [22].

$$\Delta P = -\rho W^2 \frac{\varepsilon_h}{1-\varepsilon_h} + \langle \rho\varepsilon \rangle g h - \langle F \rangle h \tag{2.21}$$

where W is the superficial liquid velocity from $W = w(1-\varepsilon)$ and F the friction body force. Gas fraction ε_h is obtained at $y = h$. Friction body force is given from $\tau_w = \frac{F}{A}$ with $A = l w_{\text{el}}$.

2.12. Semi-analytical model

Besides the numerical model, a semi-analytical model was used for comparison purposes and to initiate an analytical study for further projects. The derivation of this semi-analytical model is based on the work of [22].

For this analysis, we begin from the mass conservation of the liquid and gaseous phases separately, which are given with equations (2.22) and (2.23) respectively. To make the model simple, the mass of the liquid phase is assumed to be constant, when in reality it decreases as water molecules are electrolysed to hydrogen and oxygen molecules. At the same time, the mass of the gaseous phase is increasing at the rate given by Faraday's law of electrochemical reactions.

$$\frac{d\rho_{\text{l}}(1-\varepsilon)}{dz} = 0 \tag{2.22}$$

$$\frac{d\left(\rho_{\text{g}}\varepsilon(w+w_{\text{s}})\right)}{dz} = \frac{jM}{N_{\text{el}}Fl} \tag{2.23}$$

The differences between the numerical and analytical models are in the following equations. Firstly, the gas mass conservation equation (2.23) is integrated to obtain the gas fraction profile across the width of the electrode gap. The gas mass is integrated along the electrode surface, from $z = 0$ to $z = h$, assuming constant current density $j = constant$ and no-slip velocity $w_{\text{s}} = 0$. The result is given in equation (2.24).

$$\varepsilon = \frac{1}{1 + \frac{\rho_{\text{g}} FWln}{Mjz}} \tag{2.24}$$

For the average gas fraction, equation (2.24) is integrated again along the electrode height and divided with the electrode height to obtain the average value. The result is given in equation (2.25).

$$\langle \varepsilon \rangle \approx \frac{1}{1 + \frac{W\rho_{\text{g}} nFl}{jMz\phi}} \tag{2.25}$$

Similarly, the average friction body force $\langle F \rangle$ is obtained by averaging over the electrode height. Friction body force is again given by the Hagen-Poiseuille model for laminar flow and Darcy-Weisbach model for turbulent flow. The result is given in equation (2.26).

$$\langle \frac{2Fh}{\rho_l W_c^2} \rangle \approx \begin{cases} \bar{W}\bar{k}_1 \left(1 + \frac{1}{\bar{W}} + \frac{1}{3\bar{W}^2}\right) (laminar) \\ \bar{W}^2 K_1 \left(1 + \frac{1}{2\bar{W}}\right) (turbulent) \end{cases} \tag{2.26}$$

We then arrive at the same form of the momentum equation, which is given below in equation (2.27):

$$\rho\langle\varepsilon\rangle g h = \frac{\rho W^2}{2}\left(\frac{\varepsilon}{1-\varepsilon} + \frac{K_2}{1-\varepsilon} + K_3\right) + \langle F \rangle h \tag{2.27}$$

The advantages of analytical studies are the main initiative for this effort. To name a few, an analytical model is exact, instant to generate values, has no stability issues, it is better for sharing with other people and for improvements.

3

Methods

3.1. The research question

What are the optimal dimensions for the piping network of a water electrolysis system, for maximum flow velocity or volumetric flow rate of the liquid mixture? Developing a tool in Python that estimates the recirculation flow velocity, for a given geometry, in a natural convection alkaline electrolyser in 1D.

3.2. Geometry

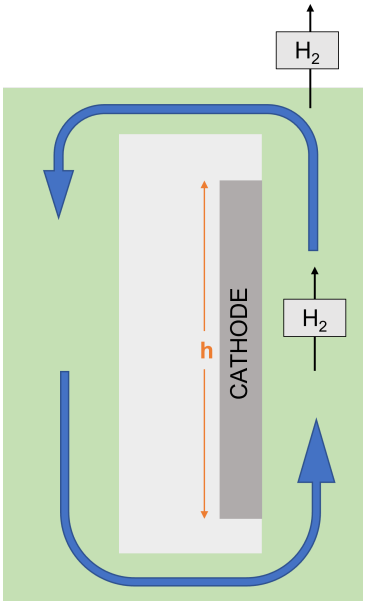

Figure 3.1: Single cell geometry. The flow channel is indicated with green colour. On the left column, the electrolyte flows downwards whereas on the right column, hydrogen evolution occurs on the cathode and gas-liquid mixture flows upwards. In the top right corner, ideal separation of the gas is assumed. The flow and geometry in the figure resembles half of an electrolysis cell. On the other half a mirrored geometry and flow occurs, with the anode and oxygen.

Four different geometries were investigated during the current study. The difference between the geometries is on the piping network which makes the system, on the number of cells and on the stacking arrangement. For each geometry, the flow on the cathode side is investigated. During water electrolysis, the gas evolving on the cathode is hydrogen. Therefore, the assumed gas density and viscosity are equal to hydrogen's.

The first geometry is the cell geometry and it is defined from a rectangular loop, which resembles the flow channel. On the right vertical section as it is illustrated with the schematic in figure 3.1, on the

cathode surface hydrogen bubbles evolve. As a result, flow occurs in a clockwise direction in the flow channel.

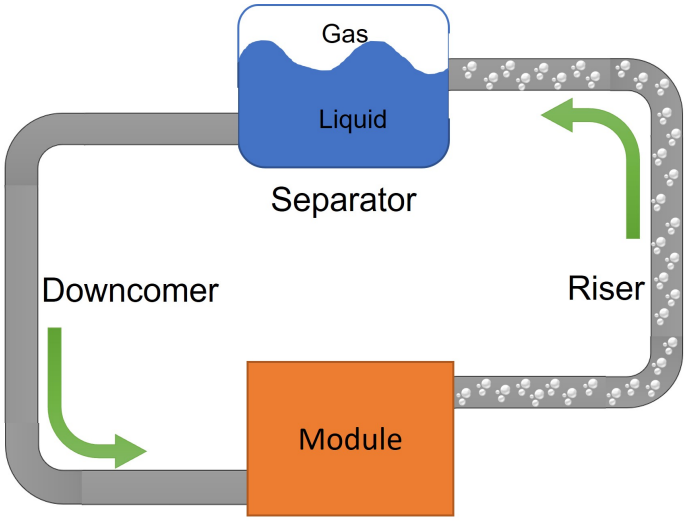

Figure 3.2: A single electrolysis module geometry with one or multiple cells within the module. The flow loop includes the separator tank, the downcomer, the electrolysis module and the riser. Here only on set of downcomer and riser are shown for illustration purposes, which are necessary for the cathode side of the system. Another set of pipelines and separator is required for the flow through the anode side and oxygen-electolyte mixure.

The next step was to extend the geometry and include longer pipe sections. The second geometry is the single modle geometry, which is a more realistic setup, as it includes multiple cells and external flow channels. In figure 3.2, the geometry is illustrated. For a natural convection system, the height of the downcomer and riser columns are important, as they can define the driving force for the flow, which is a trade-off between hydrostatic pressure difference and frictional pressure drop. The hydrostatic pressure difference is defined as the difference between the pressure in the downcomer and the pressure in the riser columns, due to the gravitational force on the fluid mixture.

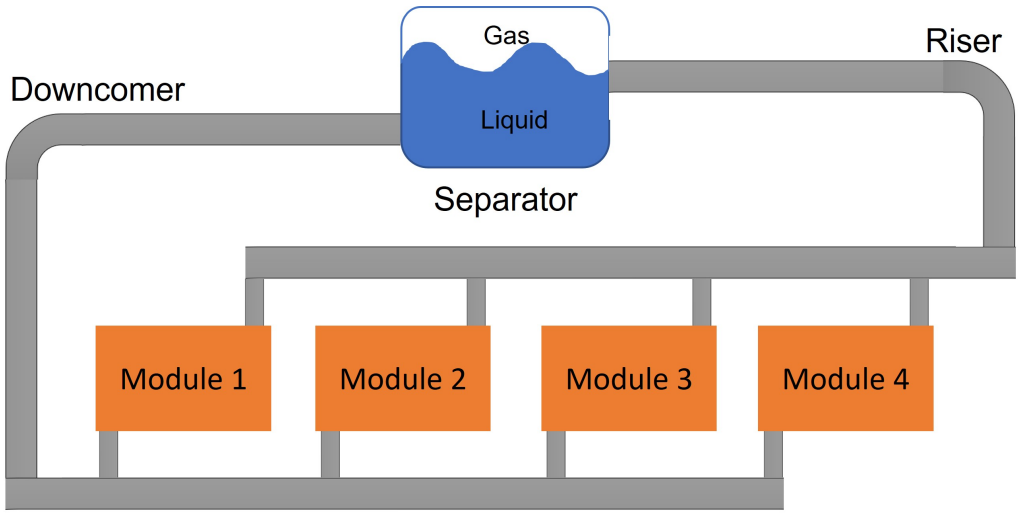

Figure 3.3: Horizontally stacked geometry of four identical modules, each module includes the same number of cells. The flow rate through the downcomer, is assumed to be equally divided into the four modules and then combined in the riser.

For the third geometry, four modules are stacked on the same level, illustrated in figure 3.3. The purpose of this model is to study the effect of the added pipe network that is responsible for dividing the flow into a number of modules. The geometry assumes that there are four modules with the same number of cells. This additional divider is called a manifold. In the geometry, an inlet manifold divides

the flow into four modules and a collector manifold combines the four parts of flow into one.

The mass flow rate, of electrolyte liquid, through each one of the four modules, was assumed to be equal, as equation (3.1) indicates.

$$\dot{m}_1 = \dot{m}_2 = \dot{m}_3 = \dot{m}_4 = \dot{m}_{\text{module}} \tag{3.1}$$

Therefore, the volumetric flow through the downcomer and riser columns is given by the summation of the four parts, as it is shown with equation (3.2).

$$\dot{m}_{\text{downcomer}} = \dot{m}_{\text{riser}} = \dot{m}_1 + \dot{m}_2 + \dot{m}_3 + \dot{m}_4 = 4 \times \dot{m}_{\text{module}} \tag{3.2}$$

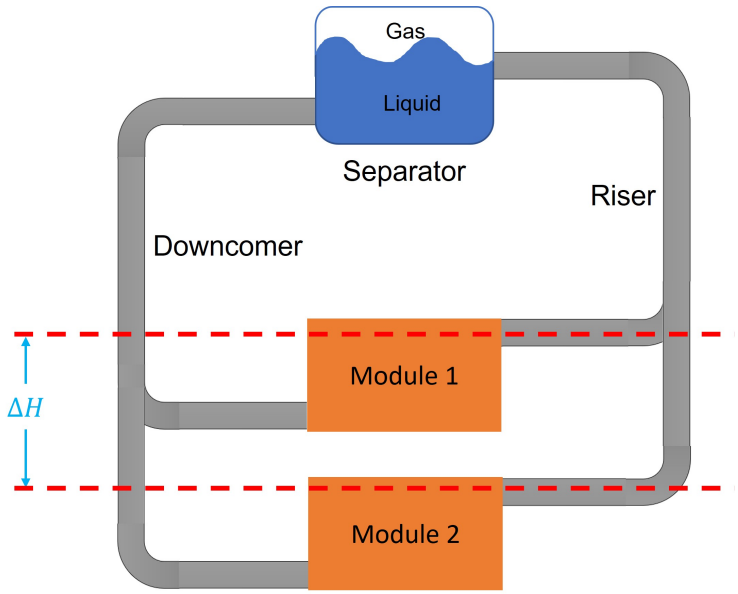

Figure 3.4: Vertically stacked geometry with two modules of the same number of cells.

The fourth geometry, found in figure 3.4, has two modules stacked one on top of each other, thus it is called vertically stacked geometry. The modules have an elevation difference Δh and the purpose is to investigate its effects on the flow. Similarly to the horizontally stacked geometry, two manifolds are responsible for dividing and combining the flow, before and after the electrolysis modules.

3.3. Running the simulations

To obtain results, the simulations are conducted using a Python code, developed for this study. In the code, the numerical model, which is a momentum conservation equation, is solved for flow velocity. A minimize function is employed and minimized the momentum balance on the second power. This is the objective function and it is given with equation (3.3). The value of flow velocity that satisfies the objective function, is the solution.

$$\left(\langle \rho \varepsilon \rangle g h - \Delta P - \rho W^2 \frac{\varepsilon_h}{1 - \varepsilon_h} - \langle F \rangle h \right)^2 = 0 \tag{3.3}$$

The value of flow velocity of the electrolyte through the electrode gap width was predicted, by varying one parameter of the model at a time. The parameters that were varied are:

- Electrode gap width
- Current density
- Electrode height
- Downcomer diameter
- Number of cells per module

4

Simulations

4.1. Validation

This section explains the process for the validation of the code. For the validation, two papers were studied and compared to the results produced by the current study. Simultaneously, a semi-analytical model was developed following the method in ref. [22].

4.1.1. Hine and Murakami 1980

In this paper, the effect of bubbles on the electrical resistance is experimentally measured. The setup from ref. [23] included a vertical cell with a single electrode. The dimensions of the electrode was 89 cm in height and 3 cm in width and the electrode gap was adjustable, with the help of interchangeable spacers which had widths between 0.5-3 cm. The design of the cell is illustrated with figure 4.1.

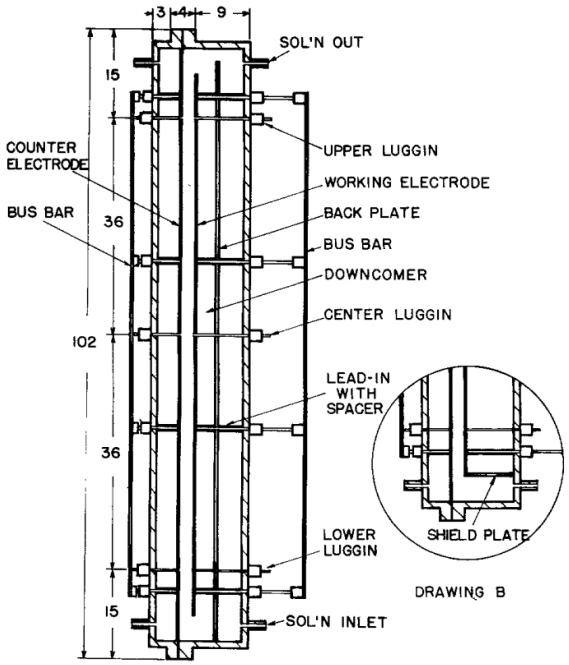

Figure 4.1: Experimental setup of a vertical electrolysis cell, used for the measurements of IR drop from [23]. The inter-electrode gap width can be adjusted between 0.5 and 3 cm, by changing spacers between the electrodes. The height of the electrodes are fixed at 89 cm and the width at 3 cm.

The experiments were carried out both for free and forced convection flows. The experimental setup had the following similarities to the geometry investigated in the current study:

- Free convection: Free or natural convection is identified by the absence of an external pumping force. Then, the liquid flow is depending only on the buoyancy effect due to density difference between riser and downcomer.
- Distributed bubbles: A few characteristics of the experimental setup suggest that the gas bubbles were not contained in a thin layer next to the electrode surface. Instead, the bubbles were distributed in the electrode gap because of the height, which is 89 cm and it is considered tall. The second characteristic is the high current densities between 750 A/m^2 and 3720 A/m^2. Furthermore, Hine and Murakami observed in most of the experiments, that the flow pattern was clearly a dispersion of gas bubbles.
- Rectangular flow channel: The geometry of the channel that is available for the liquid to flow through has a rectangular path geometry and a rectangular cross-section. Moreover, the gas is able to escape at the top of the riser column.

Taking into consideration the similarities listed above, the results from the experiments were considered interesting for validating the model developed for the current project, with a few adjustments in the numerical model. The flow velocity in the electrode gap width as a function of the gap width was the relation that was investigated.

The results given in [23] were compared to the results of the current study for validation purposes. More specifically, the simplified cell geometry is equipped for the comparison with the turbulent flow model, since the flow will be almost certainly turbulent. The parameters that are implemented to simulate the experiment, are listed below on table 4.1:

Description	Symbol	Value
Liquid density	ρ_{liquid}	997 kg/m^3
Liquid viscosity	μ_{liquid}	2.04 $\times 10^{-3}$ $Pa \cdot s$
Gas density	ρ_{gas}	0.0813 kg/m^3
Gas viscosity	μ_{gas}	8.92 $\times 10^{-6}$ $Pa \cdot s$
Electrode height	h	89 cm
Electrode width	w_{el}	3 cm
Gap width	l	0.68, 1.47, 1.97, 2.50 cm
Current density	j	3720, 2270, 750 A/m^2
Temperature	T	40 °C
Pressure	p	1 atm
Friction factor	K_2	1.0
Friction factor	K_3	0.9

Table 4.1: Values for the validation with the experimental results from ref. [23].

The dimensions are implemented in the code as shown above. In the geometry of the current study, the electrode gap refers to half of the anode-cathode distance. Since the experimental geometry lacks a separator, the flow channel is equal to the inter-electrode distance. Therefore, the inter-electrode distance from the reference article was used as the electrode gap for the simulation. Moreover, to account for both the hydrogen and oxygen in the flow, a current density equal to 75% of the experiment's current density and a number of electrons $N_{\text{el}} = 4/3$ for Faraday's law in equation (1.1). This is because the volume of evolved oxygen is half of the hydrogen volume, and in oxygen evolution one electron is involved. The relation of current density, is explained below with equation (4.1).

$$j_{\text{simulation}} = 3/4 \times j_{\text{experiments}} \tag{4.1}$$

The results from the paper are illustrated in figure 4.2 alongside the results from the numerical model for the cell geometry.

From figure 4.2, we can observe that the simulation predicts values of flow velocity, two times as big as the values from the experiments. This indicates that the hydrodynamic friction in the geometry is too little or the amount of evolved gas is more than in reality, or both. Besides, we observe a similar profile of velocity, with higher magnitude, which is a signal that the behaviour of velocity as a function of current density is similar to the experiments. Moreover, the researchers experimented with the

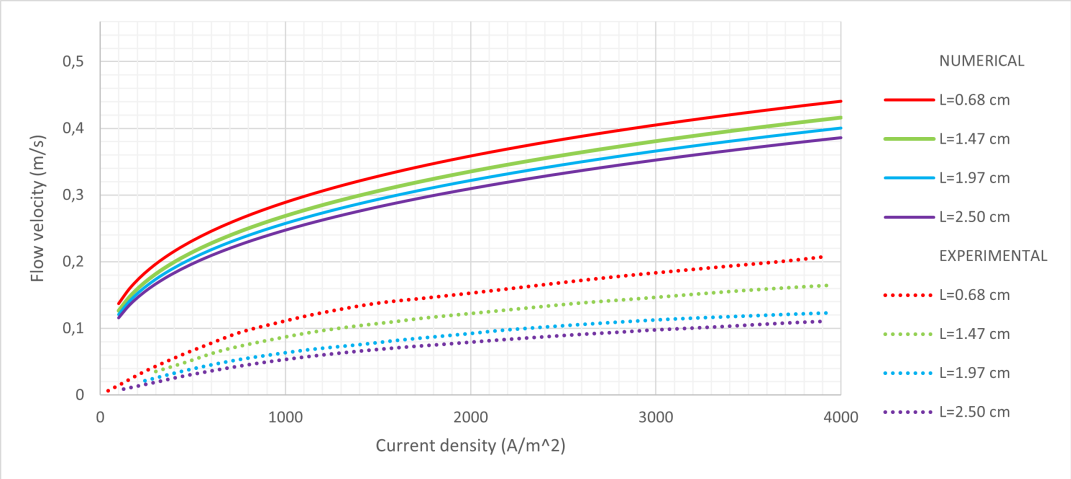

Figure 4.2: Circulation velocity in the gap width as a function of current density. Each curve represents a different electrode gap. The numerical solution is calculated with the turbulent flow model and it is shown together with the experimental results from ref. [23].

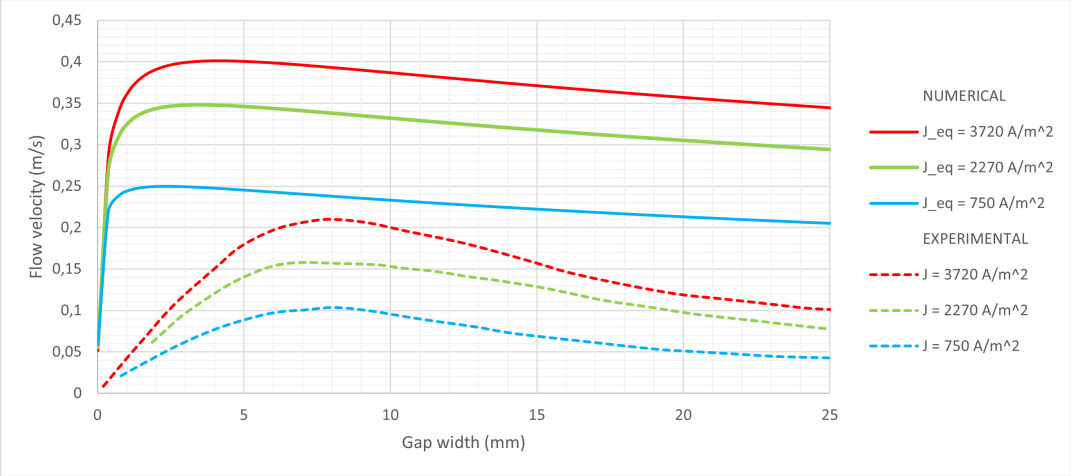

Figure 4.3: Circulation velocity in the gap width as a function of current density, curves for various gap width values. The figure includes results from the laminar flow model, the turbulent flow model and from experiments found in ref. [23].

effect of gap width on the circulation velocity. They obtain data for three values of current density, $j = 3720,\ 2270,\ 750\, A/m^2$. The comparison is given with figure 4.3.

In figure 4.3, there is again an over-estimation of the magnitude of flow velocity. This can be explained with the same reasons as it was explained for comparison in figure 4.2. The current profile gives as an additional observation. Specifically, the maximum points of the velocity profile are found at lower gap widths relative to the experimental results. These maxima correspond to the optimum gap widths for each current density curve. This indicates that the actual optimum points are at higher electrode gap widths than what the model predicts.

4.1.2. Rousar 1987

From the paper of Rousar, the experimental results for flow velocity in the gap width as a function of current density were simulated. The experimental setup is illustrated with figure 4.4. The single module geometry model was employed with the turbulent flow model because the geometry with riser and downcomer is more relevant to the experimental setup and the flow is almost certainly in the turbulent region. In the module one electrolysis cell is assumed. The heights of the downcomer and riser represent the pumping height Δl, as it is defined in the reference paper. For each curve on the figure, a different value of Δl is assumed. Four different values were tested: $40,\ 80,\ 160,\ 240$ and $320\ mm$. For the simulation, the parameters on table 4.2 were used.

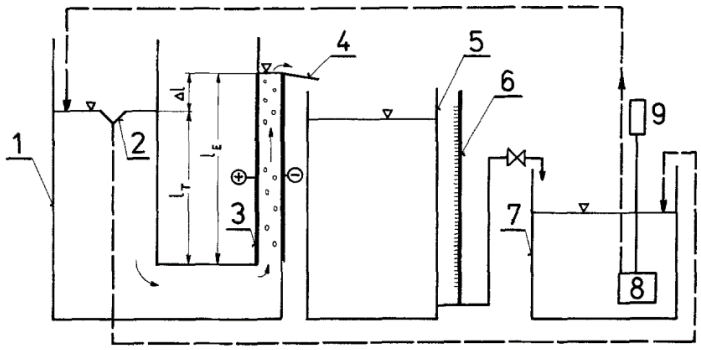

Figure 4.4: Experimental setup used from ref. [24]. On the schematic, the number 3 indicates the location of the electrodes and the electrode gap with the bubbly mixture.

Description	Symbol	Value
Liquid density	ρ_{liquid}	997 kg/m^3
Liquid viscosity	μ_{liquid}	2.04 $\times 10^{-3}$ $Pa \cdot s$
Gas density	ρ_{gas}	0.0813 kg/m^3
Gas viscosity	μ_{gas}	8.92 $\times 10^{-6}$ $Pa \cdot s$
Downcomer height	h_{D}	40, 80, 160, 240, 320 mm
Electrode height	h	70 cm
Electrode width	w_{el}	13 cm
Gap width	l	6 mm
Current density	j	100 - 9000 A/m^2
Temperature	T	40 °C
Pressure	p	1 atm

Table 4.2: Parameters implemented for the validation with experimental results from ref. [24].

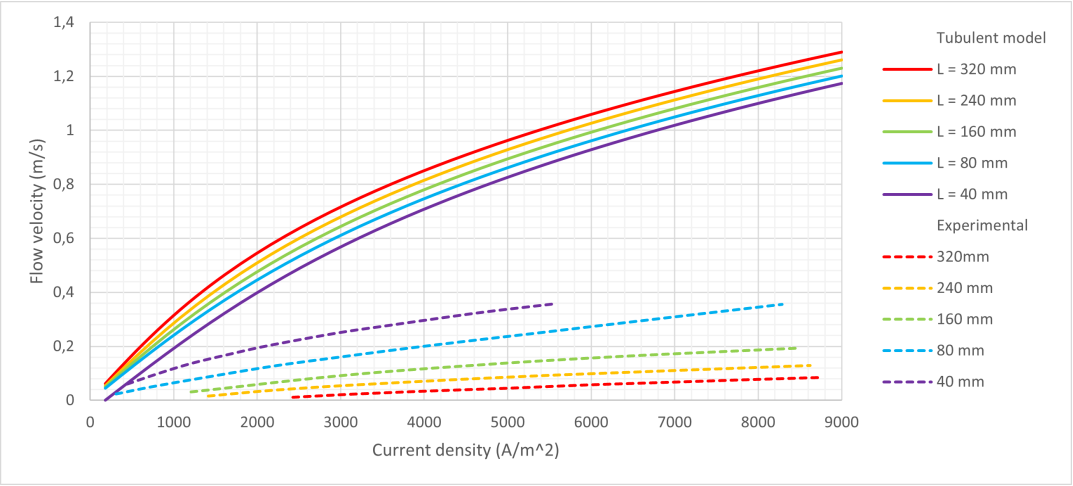

Figure 4.5: Flow velocity in the electrode gap as a function of current density, a comparison of solutions with turbulent model and experimental data from ref. [24]. Each curve represents a different value of pumping height, which is equal to the downcomer and riser height, creating a pumping effect with the buoyancy force.

The results of the simulation show that the numerical model predicts higher flow velocities in the electrode gap. The difference in velocity magnitude is approximately a factor of 6. This indicates that again the predicted friction is lower than in reality and the evolved gas is overpredicted. An important observation is that, the experimental results show that flow velocity increases as the pumping height decreases. In contrast, the simulation predicted that the flow velocity increases as the pumping height increases. This indicates that the numerical model may overlooks an important effect that is included in

the experiments from ref. [24].

4.2. Semi-analytical model

As it was explained in the methods chapter, a semi-analytical model was derived and compared to the numerical model. The two models were used in a simulation which returned predictions for the gas fraction profile in the cell geometry. On figures 4.7 and 4.6 a comparison is given of the two models.

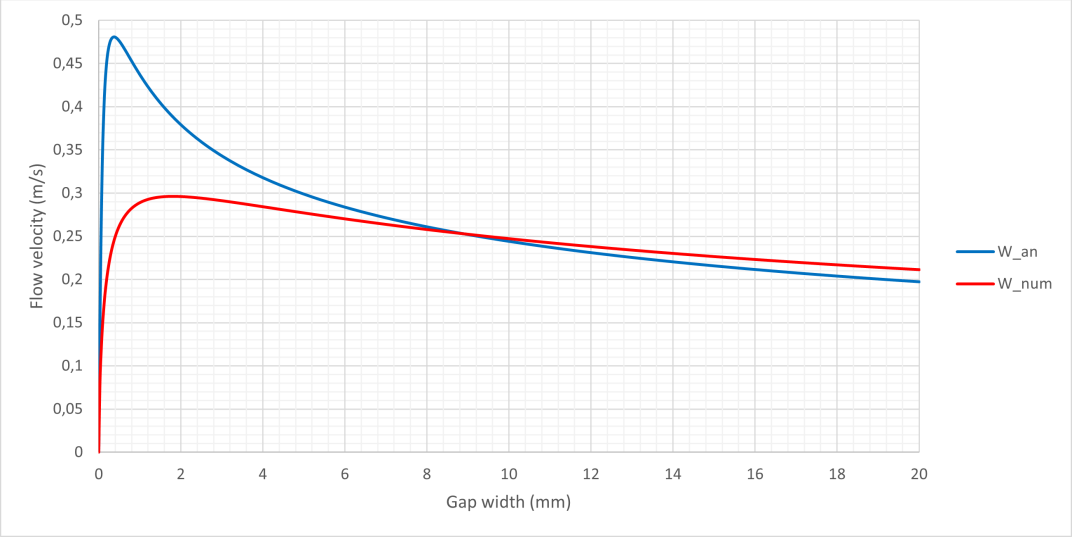

Figure 4.6: Flow velocity as a function of gap width, at constant current density $j = 10000\ A/m^2$. A comparison between numerical and semi-analytical models.

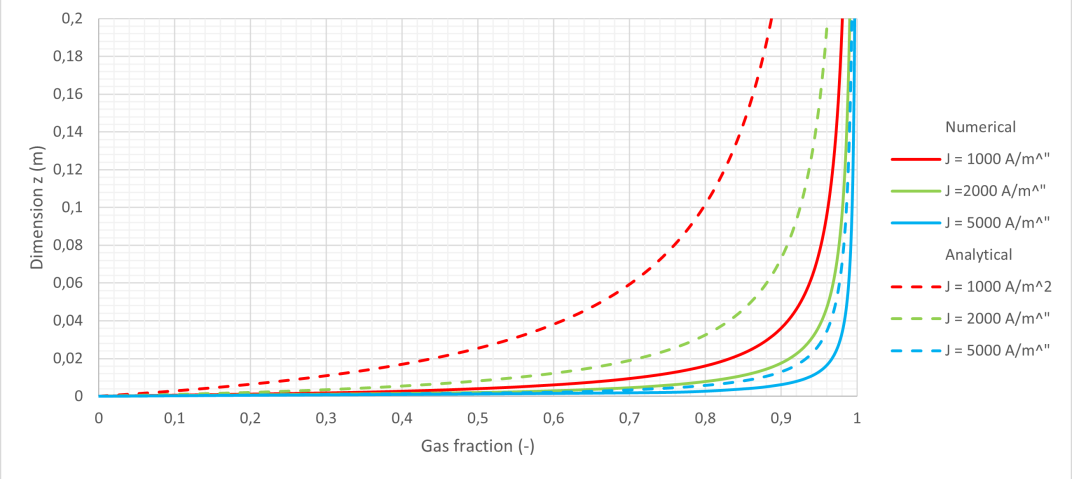

Figure 4.7: Gas volume fraction profile in the cell geometry. A comparison between numerical and semi-analytical models.

Both the results of gas fraction in the gap width and the results for flow velocity as a function of gap width agree that the semi-analytical model predicts higher velocities for the same current density and gap width. This can be observed clearly by the values on figure 4.6 where the curve for the semi-analytical solution is above the curve for the numerical model for most of the gap width values. In addition, on figure 4.7, the semi-analytical model predicts lower gas fraction values in the electrode gap compared to the numerical model. Consequently, the conclusion is that there is less accumulation of gas bubbles in the electrode gap due to the higher flow velocity. On the other hand, the numerical model is predicting a physical representation of the gas fraction profile in the electrode gap width and gives a shows a maximum point for flow velocity, which are both expected.

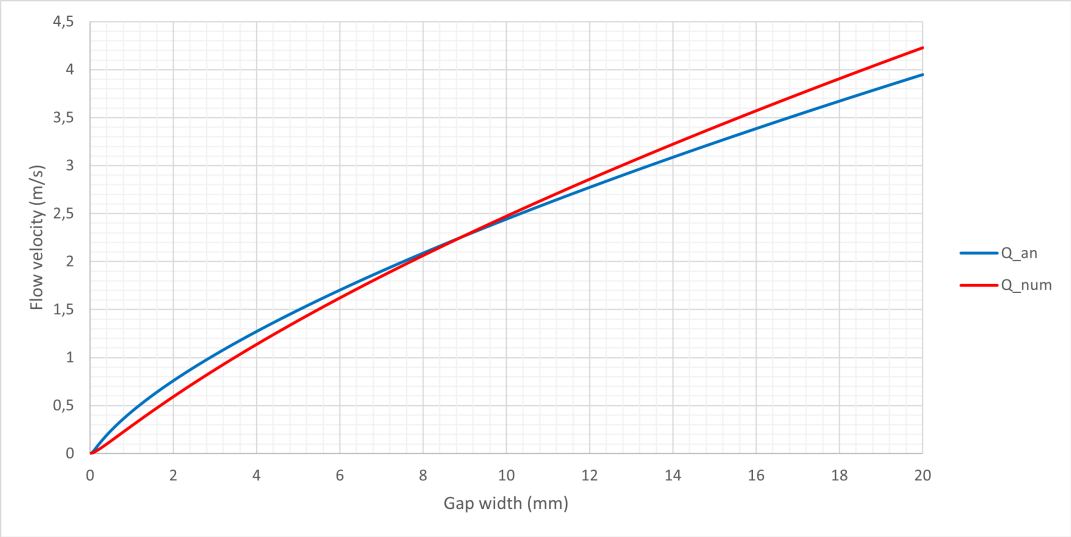

Figure 4.8: Flow rate as a function of gap width, at constant current density $j = 10000\ A/m^2$. A comparison between numerical and semi-analytical models.

4.3. Sensitivity analysis

The purpose of sensitivity analysis is to establish a set of operating conditions for the single module geometry, as a reference point. Then, compare the results with different geometries. At the same time, the operating conditions and electrode dimensions are defined during this step. Therefore, the following parameters are studied:

- Current density: The range found from literature. Both [25] and [26], suggest that the current density of alkaline electrolysers for industrial purposes, is between $2000 - 4000\ A/m^2$.
- Electrode height: 4 to 15 cm. Suggested by XINTC as the company is interested in more compact cells.
- Electrode gap width: 1 to 20 mm. The gap maintained above 1 mm to avoid phenomena studied only in zero-gap and nearly-zero gap cells studied by [8]. The main interest is in the lower end of the range, since ohmic losses due to the electrolyte resistivity increase with the inter-electrode distance.

4.4. Current density

The second study on the single module geometry is focused on current density. It is an important parameter for the system, because current density :

- affects the efficiency of the system. The higher the current density, the lower the electrical efficiency, the higher the production rate and the higher the gas crossover between the anode and cathode. For the current study, the current density is only investigated for its effect on flow velocity.
- is synonymous with gas evolution. The higher the current the higher the gas production and usually the higher the gas fractions in the riser column.
- affects the electrical efficiency. For higher current densities, higher voltage is required, which results in more ohmic losses.
- affects the gas cross-over. By increasing the current density, the gas fraction increases in the electrode gap. As a consequence, the mass transfer of gas molecules between the anode and cathode happens at a faster rate. Thus, by increasing current density, the danger of hydrogen gas crossing the separator and creating an explosive mixture is higher.

4.5. Downcomer diameter

For the downcomer, the diameter is studied with respect to the hydraulic friction. The friction is illustrated with flow velocity, therefore the diameter for which the flow velocity becomes independent

is selected for further studies.

The downcomer column is the piping section which connects the gas/liquid separator tank and the electrolysis cells. Through this column, the pure electrolyte is flowing downwards and enters the cells, where water electrolysis occurs. The height of the downcomer and riser are approximately equal, and the hydrostatic pressure difference between the two columns is the driving force of the flow. Therefore, the higher the two columns, the greater the driving force. In contrast, the height of the columns can not increase indefinitely, as the hydrostatic losses are also increasing. Consequently, the height is fixed to 1 meter, which is also a practical height as the system needs to be enclosed within the limits of a transporting container. On the other hand, the dimension of the downcomer diameter is more flexible, thus it is investigated in this study.

4.6. Comparison of single module geometry and stacked geometry

The last step is the comparison with variations of the geometry. The horizontally and vertically stacked geometries are possible solutions for increasing the hydrogen production rate, in a compact and cheap manner. Subsequently, an electrolyser company like XINTC, is interested in looking for the best combination of efficiency and manufacturing cost.

5 Results

The model is now employed to make observations and assist the design process of a natural-recirculation electrolysis system. For the following simulations, the flow regime is assumed laminar in the downcomer and separator and turbulent in the electrode gap width and riser.

A series of studies were conducted using the numerical model. Each study was isolating a different design aspect of the electrolysis system. The parameters are given below with table 5.1. The gap width and electrode height are the most important parameters because they are impossible to vary after the electrolysis system is manufactured. At the same time, they have the most influence on gas crossover and cell voltage, which are crucial values for the safety and financial feasibility of the system.

Description	Symbol	Value
Downcomer diameter	D_D	57.4 mm
Current density	j	0 - 5000 A/m^2
Electrode height	h	10 cm
Electrode width	w_{el}	20 cm
Temperature	T	330 K
Pressure	p	1 atm
Gap width	l	0.5 - 20 mm
Liquid density	ρ_{liquid}	997 kg/m^3
Liquid viscosity	μ_{liquid}	2.04 $\times 10^{-3}$ $Pa \cdot s$
Gas density	ρ_{gas}	0.0813 kg/m^3
Gas viscosity	μ_{gas}	8.92 $\times 10^{-6}$ $Pa \cdot s$

Table 5.1: Simulation parameters.

5.1. Comparison of optimum points

This simulation is about comparing the optimum gap widths for different current densities, employing the single module geometry with one cell in the module. The gap width was varied between 0.5 mm and 20 mm while the current density took values of j = 500, 1000, 2000, 4000, 8000 and 16000 A/m^2. The results of the simulation are given in figure 5.1. The curves are reduced to a gap width range between 0.2 mm and 5 mm, to make the difference between the optimum points clearer.

5.2. Minimum downcomer diameter

The downcomer column is a column of pure electrolyte, and the velocity through this column should be as low as possible to minimize hydrodynamic pressure losses. At the same time, the dimensions of the pipe sections need to be relative small to keep the material cost and the size of the electrolyser system small. To approach this task, the flow velocity through the cell is examined as a function of the downcomer diameter. The current density was kept constant at 2000 A/m^2 and electrode gap width at 5 mm.

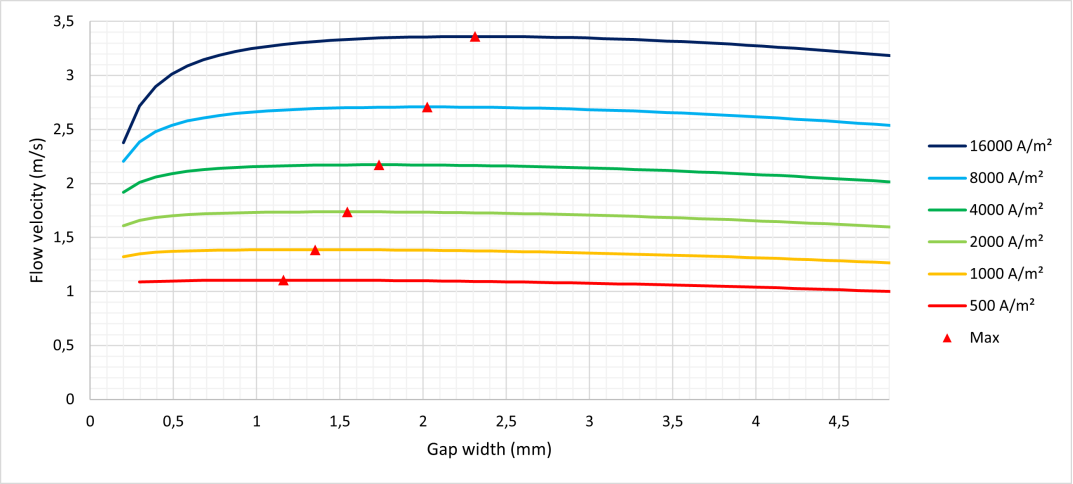

Figure 5.1: Flow velocity in the electrode gap width, as a function of the gap width. Each curve represents a different value of current density. The maximum flow velocity of each curve is indicated with a red triangle.

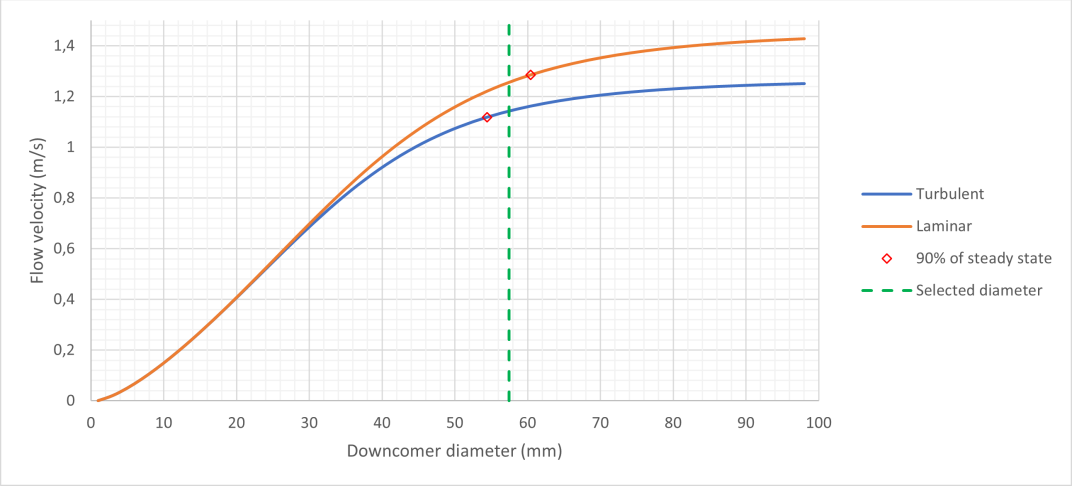

Figure 5.2: Flow velocity in the electrode gap width as a function of downcomer diameter. The values of flow velocity for the larger gap width are considered steady state. The two red markers indicate the 90% of these steady state velocities and the green dotted line show the final value which is selected as the minimum downcomer diameter which is 57.4 mm.

From figure 5.2, the flow velocity becomes independent of the downcomer diameter at approximately 90 mm. For downcomer pipes with larger diameters, the flow velocity is considered constant. The steady state velocity for the turbulent model is 1.13 m/s and for laminar model is 1.29 m/s which correspond to 54.4 mm and 60.4 mm of diameters, respectively. To choose the minimum value of the downcomer diameter, the 90% of all steady flow velocity values are select. This percentage ensures that the hydrodynamic friction in the downcomer is of smaller significance, and at the same time the downcomer is kept relatively compact.

As a result, the selected minimum downcomer diameter is 57.4 mm. For a real word application, a standardized diameter will be selected. The smallest diameter above 57.4 mm is recommended.

5.3. Current density

The effect of current density on gas fraction and mixture viscosity is investigated. The aim is to understand the relation between flow velocity and current density to aid the design process of an electrolysis system.

In figure 5.3, the results for this study are illustrated. The plot represents the value of flow velocity W as a function of current density j. Each curve represents the solution for a different number of cells per module. For example, the orange curve represents an electrolysis system with a single module

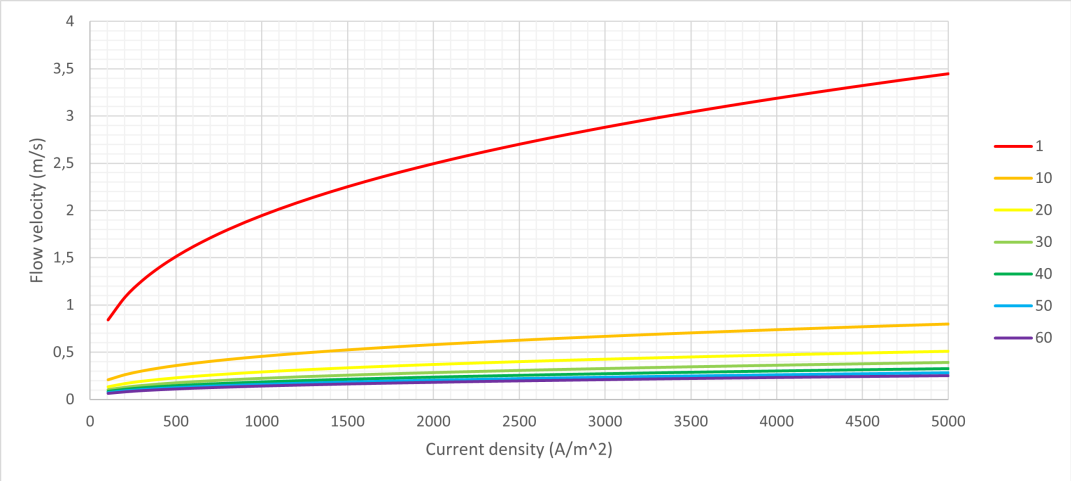

Figure 5.3: Flow velocity in the electrode gap as a function of current density. Each curve represents a different number of cells in the module.

which includes 10 electrolysis cells.

Observing figure 5.3, the results suggest that the flow velocity is increasing with increasing current density. The same conclusion is given observing flow rate in figure 5.4. Therefore, a common value for current density is chosen for the following studies. The reason is that, there is no maximum point of flow velocity or flow rate. Also, the current model will predict higher flow velocities for higher current density, since the effect of ohmic losses are not included. Therefore, selecting an extremely high value for current density will not be realistic. The selected value is 2000 A/m^2, which is in the lower end of the current density range for alkaline electrolysers, as it is suggested by [25] and [27].

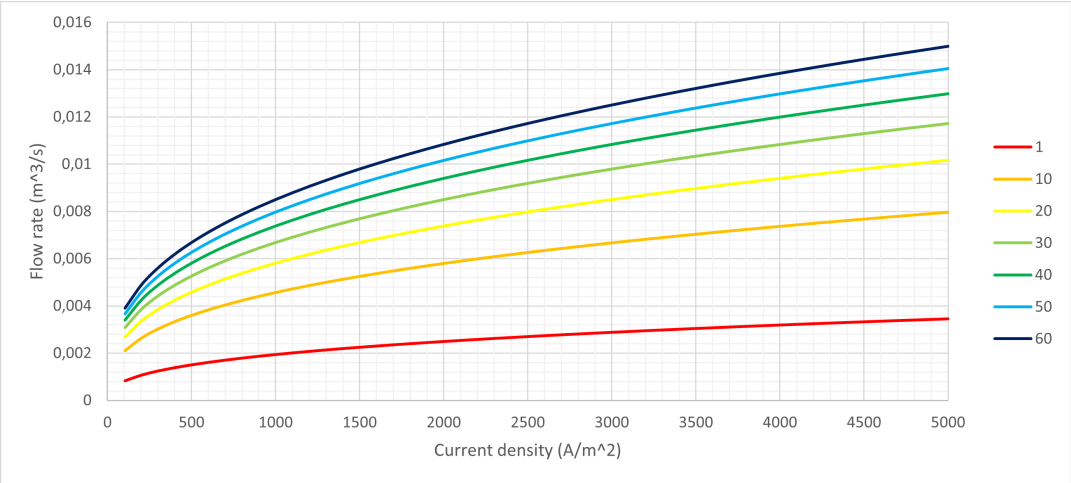

Figure 5.4: Total volumetric flow rate as a function of current density. Each curve represents a different number of cells in the module. The volumetric flow rate is calculated by multiplying the velocity, the number of cells, the electrode width and the electrode gap.

As shown, there are two methods to increase gas fraction in the riser column. As it was explained, the riser is where the total flow passes and the gas fraction in this column, is directly related to the driving force and the resistance for the flow. One way of increasing the driving force is by increasing the gas fraction. Then, two methods are available to increase gas fraction. The first one being to increase current density and the second to increase the number of cells. Consequently, number of cells and current density are two important design parameters that affect flow velocity and volumetric flow rate.

5.4. Electrode height

Electrode height refers to the vertical dimension of the electrodes and it is important since it affects the effective electrolysis area. Increasing the electrode height can increase the gas fraction, thus the flow velocity and at the same time increase the gas cross-over. For this study, electrode height is investigated only as a mean to optimize the system for flow velocity.

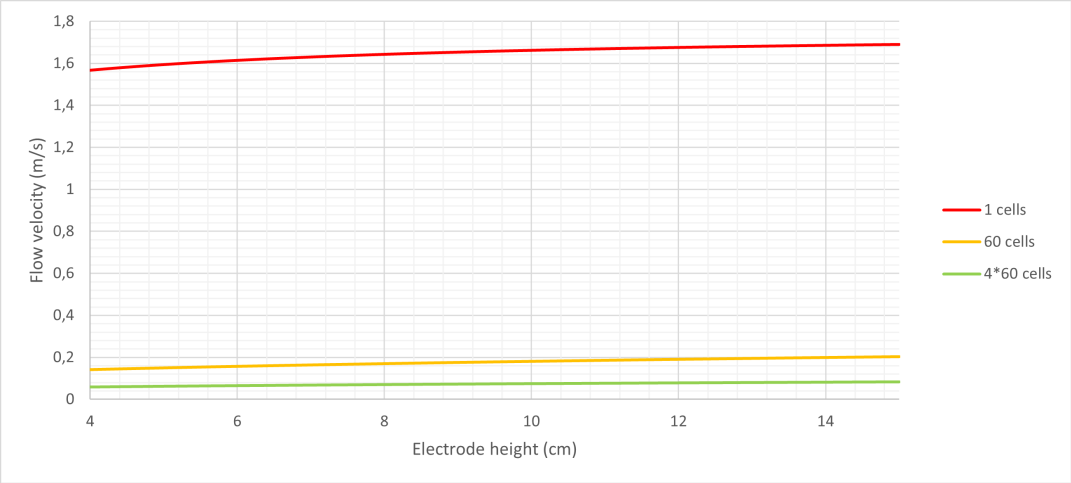

Figure 5.5: Flow velocity in the electrode gap width as a function of the electrode height. The current density is kept constant at 2000 A/m^2. Each curve represents a different number of electrolysis cells in the module. An electrode height of 10 cm was selected for the rest of the simulations.

From figure 5.5 we can observe that for increasing electrode height, the flow velocity increases. Therefore, the maximum electrode height is given taking into account the calculation of gas crossover, which is not a part of the current model. For the purpose of the current model, a value of 10 cm is selected for electrode height.

5.5. Gap width

In the presence of a diaphragm, the distance between the electrode to the diaphragm is call gap width. For a gap with pure electrolyte the conductivity increases as the gap is getting wider. Simultaneously, as the gap is getting narrower, the friction to the flow increases the gas fraction is increasing. The current study, examines the balance between the driving force and the friction losses, to arrive at suggestions for the electrode gap width.

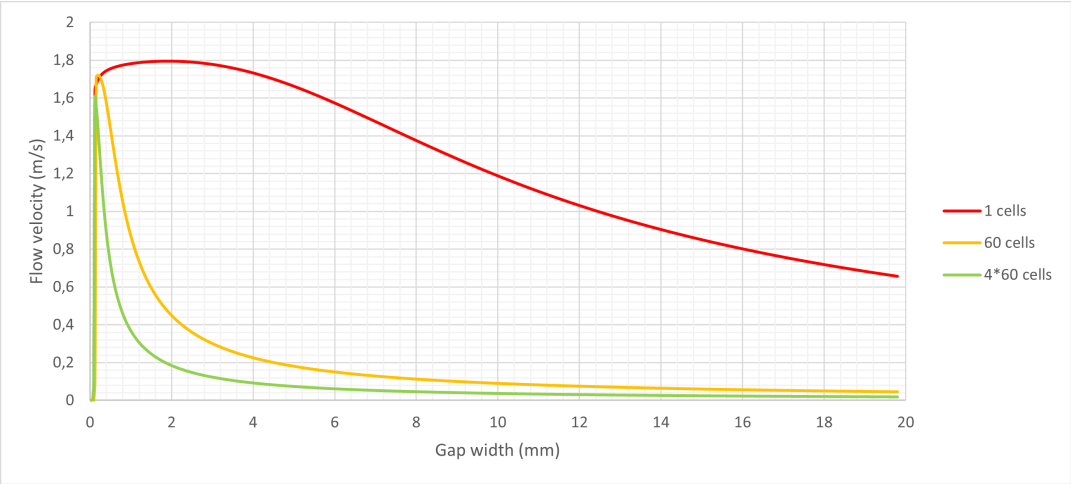

Figure 5.6: Flow velocity in the electrode gap width as a function of the gap width. Each curve represents a different number of electrolysis cells in the module.

The optimum gap width, is found at the point where the balance of friction losses and gas fraction result in maximum flow velocity. This relation is illustrated with figure 5.6, which gives the solutions with the laminar flow model. Each curve has a maximum point. This point corresponds to maximum flow velocity and happens at the optimum gap width value. The values of the optimal gap widths as predicted with the numerical model, are given in table 5.2.

Number of cells (-)	Flow velocity (m/s)	Gap width (mm)
1	1.8	1.9
60	1.7	0.25
240	1.3	0.25

Table 5.2: The electrode gap widths for which we get a maximum flow velocity in the gap width. Each value is given with the predicted velocity and the number of cells assumed in the module.

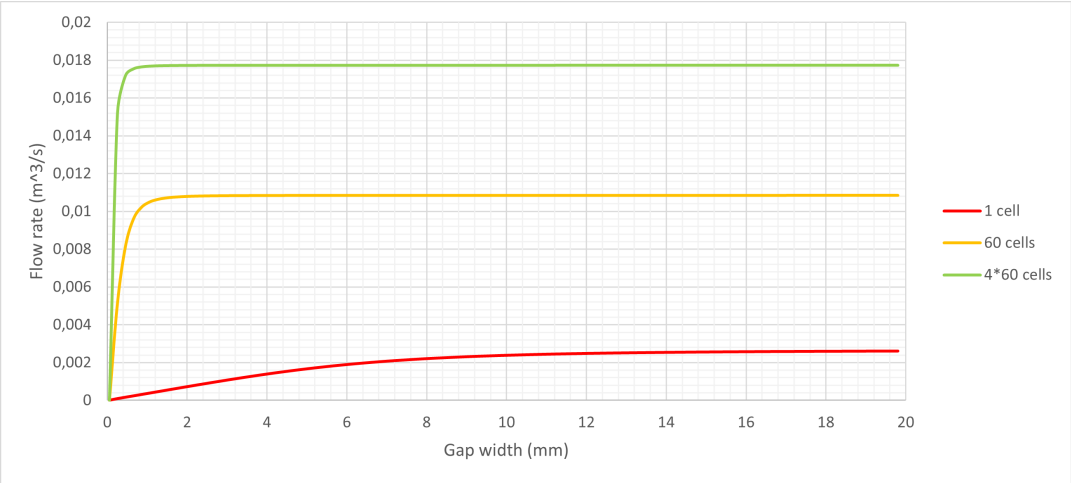

Figure 5.7: Total volumetric flow rate as a function of the gap width. Each curve represents a different number of electrolysis cells in the module.

A different relation is showed in figure 5.7, where the flow rate increases with gap width until it reaches a steady state. On table 5.3 the values of gap width for which the flow rate reaches the 90% of constant value is presented.

Number of cells (-)	Gap width (mm)
1	9.6
60	0.85
240	0.45

Table 5.3: Gap width values for which volumetric flow rate is at 90% of the constant value, for the single module geometry.

5.6. No riser/downcomer columns

For the current study, the dimensions of the riser and downcomer to include the friction losses from the piping network of a water electrolysis system. In this section, the effect of these friction losses are investigated. A comparison of the solutions in the previous section and the results excluding the riser and downcomer columns is made. The goal is to understand the effect of the additional friction and check whether the behaviour of the system changes in any way.

In figure 5.8 the solutions for the same geometry excluding the two columns are illustrated. The extended geometry with the two columns has the same behaviour when increasing the electrode gap width. Namely, the flow velocity increases to a maximum point and then decreases again. The difference is in the value of flow velocity. Even though the columns add friction to the flow, the effect of hydrostatic pressure difference is greater. As a result, an increase in the flow velocity for all cases is observed.

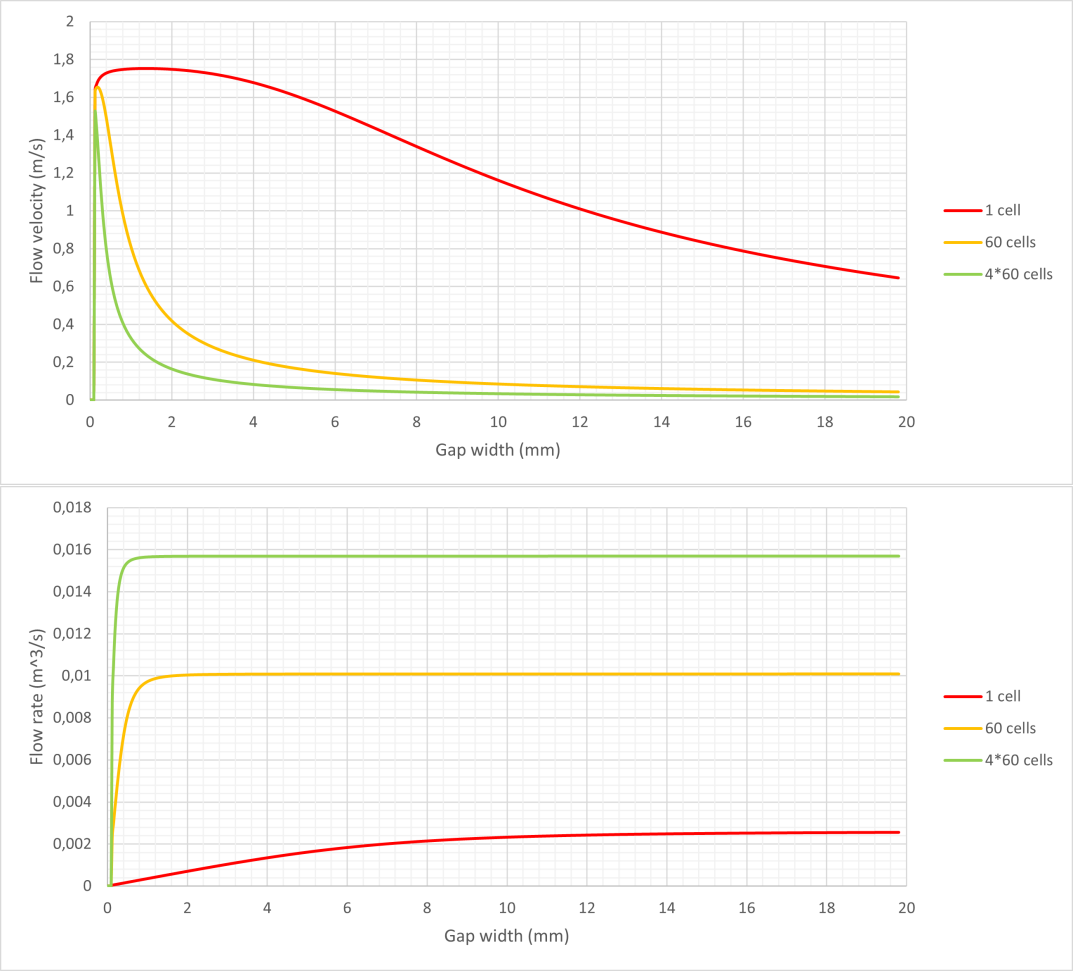

Figure 5.8: Study on the effect of riser and downcomer columns. On the top, the results for flow velocity in the electrode gap width as a function of gap width, for 1 60 and 240 cells in the module. On the bottom, the flow velocity was converted to volumetric flow rate, by multiplying with electrode width and gap width.

A comparison of figures 3.2 and 5.8 indicates a small increase, which depends on the number of cells per module. On table 5.4, the increase of flow velocity in value and percentage is given.

Number of cells (-)	Increase in velocity (m/s)	Increase in percentage (%)
1	0.042	2.4
60	0.067	4.0
240	0.084	5.5

Table 5.4: Comparison between geometry without riser and downcomer columns and single module geometry

5.7. Horizontal stacking

In this section, the effect of the horizontal stacking of modules is examined. As it was explained, four modules with the same number of electrolysis cells are stacked on the same level next to each other. The main difference to the single module geometry is the additional friction due to the manifolds before and after the modules, for dividing and mixing the flows. The results of flow velocity in the electrode gap width as a function of gap width are shown in figure 5.9.

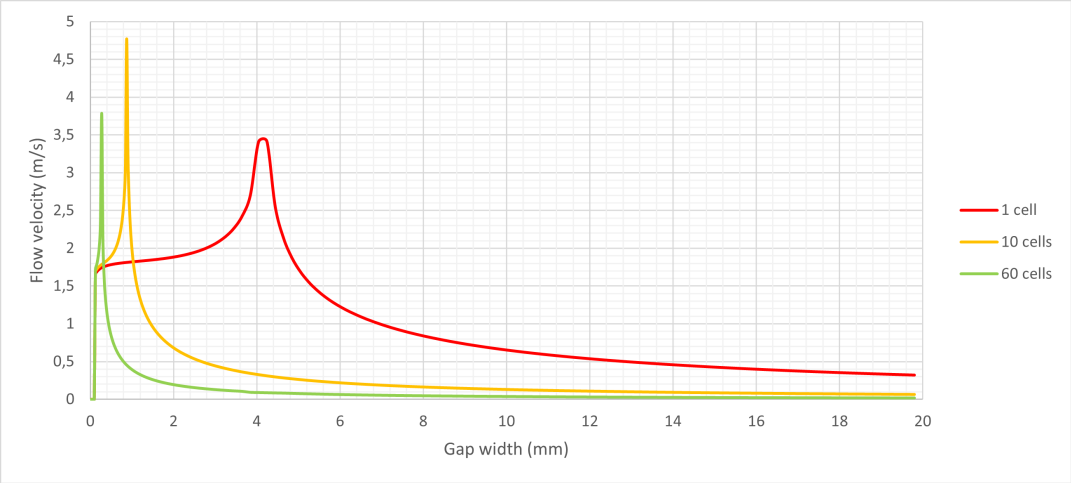

Figure 5.9: Flow velocity in the electrode gap width vs gap width with turbulent flow model. Results calculated with the horizontally stacked geometry with four modules of the same number of cells. Three curves are plotted for 1, 10 and 60 cells per modules which corresponds to 4, 40 and 240 total cells, respectively.

The maximum points, are found at high values of flow velocity and the slope of the curves near the maxima are is steep. The maximum points are listed below on table 5.5.

Cells per module (-)	Total number of cells (-)	Gap width (mm)
1	4	3.4
60	40	4.8
240	240	3.8

Table 5.5: Optimal gap width values for horizontally stacked geometry. Maximum points found in figure 5.9.

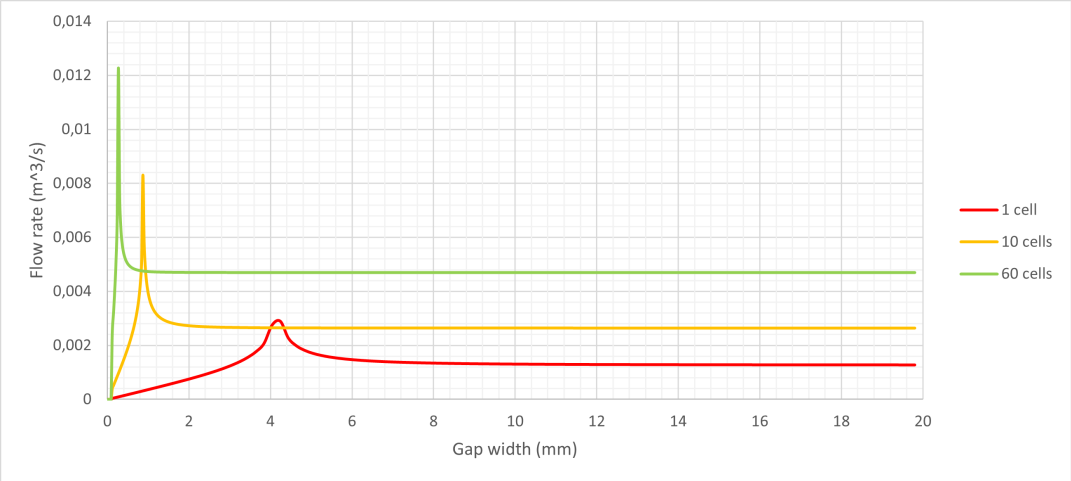

Figure 5.10: Optimal gap width values for horizontally stacked geometry. Results calculated with the horizontally stacked geometry. The values resemble the total volumetric flow rate through the cells, which is then combined in the riser.

Similarly, the curves of volumetric flow rate as a function of electrode gap width, show a high flow

velocity at the maximum points and steep slopes near them. The results for flow rate are shown in figure 5.10.

6 Discussion

6.1. Cell geometry

The single cell geometry, resembles an experimental setup that can be used for validation of the model or a geometry to be studied with Finite Element Analysis (FEA) software packages. For the current project, none of the two was made possible. Therefore, as it is explained later, validation was made by comparison to experimental results from literature.

The validation with experimental studies from ref. [23] showed a comparable behaviour of the model to the results from literature, though there were significant differences in the predicted values. The comparison in figure 4.2 showed that predicted values are two times higher than the experimental results. Comparison in figure 4.3, confirmed the same observation and showed that maximum points are predicted at narrower gap widths. The reason for the different values is that the current density for the numerical model was constant across the electrodes, whereas the current density values from the experiments may be maximum values. Consequently, more gas production is assumed for the numerical model. Furthermore, the assumption that the bubbles are distributed across the electrode gap width is not accurate. Bubbles in the experimental setup might disperse, but only after a certain height, since a boundary layer of bubbles is growing on the electrode surface. Simultaneously, the optimum gap widths were found somewhere between 0.2 and 0.6 mm, relatively to the optimum values between 0.5 and 1.0 mm from [23].

The comparison with the results from [24], showed a similar behaviour as well. The results from the current model showed higher values of flow velocity by a factor of 5, in comparison to the experimental results.

The validation process verified that the numerical model is overpredicting the flow velocity in the electrode gap and predicting narrower optimum gap width.

6.2. Semi-analytical model

The semi-analytical model assumed the same friction factors and as a result, the flow velocity in figure 4.6 and gas fraction values in figure 4.7 were similar. The most important difference was in the value of flow velocity at the optimum gap width. The semi-analytical model predicted almost twice as high flow velocity as the numerical model. Again, the two models are assuming less friction than reality. In addition, the assumption of evenly distributed gas bubbles might be an important parameter that caused such a difference.

6.3. Downcomer diameter

In figure 5.2, the results of this study, showed that as the diameter of the downcomer increases, the velocity increases. This is explained with the reduction of friction, given by the Darcy-Weisbach equation (2.15), where the characteristic length is the diameter. On the contrary, by keep increasing the diameter above a critical value, the velocity increases marginally and reaches steady state. This critical diameter is the minimum downcomer diameter, and it refers to $D = 57.4\ mm$, for the examined case.

For the downcomer diameter, we expect to see an increase in flow velocity as the diameter is increasing. This is happening because the hydrostatic pressure difference for a flow through a straight pipe is proportional to the diameter of the pipe. As the downcomer diameter increases, the aforementioned hydrostatic pressure drop becomes less significant relative to the other sources of pressure drop in the piping network. Therefore, an optimal diameter is one that results in hydrostatic pressure losses and at the same time is as little as possible to decrease the footprint of the system and the cost of materials.

6.4. Current density

The effect of current density was examined and the value was set to $j = 2000\ A/m^2$. The results, showed that the flow velocity increases as the current density increases, without any limitations. This is because the voltage efficiency as well as the mass transfer limitations are not taken into account for the current project. Therefore, a relatively low current density was chosen, within the range commonly used in the industry of alkaline electrolysers. The range found from [25] and [26] is $2000 - 4000\ A/m^2$.

6.5. Number of cells

An important observation from figure 5.3, is how the number of cells affects flow velocity in the electrode gap. As the number of cells in the module increases, flow velocity decreases. This happens because in all cases, the dimensions of riser and downcomer are the constant. Thus, the more cells the more the average gas fraction in the riser and as a result viscosity is increasing. The decrease in velocity is then explained with the increasing hydrodynamic pressure drop for increasing viscosity in the riser.

In contrast, the volumetric flow rate increases with increasing number of cells. Even though the flow velocity is the lowest for a module including 60 cells, the volumetric flow rate of the mixture through the riser is the highest. This is happening because the flow rate through each cell is added to the total flow rate, which is then recirculated through the downcomer and riser. This effect is clearly illustrated in figure 5.4.

6.6. Electrode height

The dimension of electrode height was investigated and a height of $h = 20cm$ was selected. Figure 5.5 suggests, that velocity increases as the electrode height increases. Therefore, since there is an optimum point, a relatively compact electrode was chosen. The reason is, that the taller the electrode, the higher gas crossover. Since gas crossover is not estimated by the current model, a short electrode height is a safer choice.

6.7. Single module geometry

The geometry with a single module, combined with downcomer and riser columns, acted as a reference point for the project. The results with this geometry are compared with the other geometries.

At this point, it should be disclaimed that the single module geometry was planned to be validated with experiments. Unfortunately, due to The second geometry, identified as *single module geometry*, is a more realistic approach to a full sized industrial electrolyser setup. Unfortunately, there was not enough time and resources to prepare and run an experiment for validation. Thus, the results are expected to give the behaviour of a real electrolysis system and not exact values.

6.8. Without riser and downcomer columns

Riser and downcomer columns are critical parts of the geometry because the hypothesis was about finding the dimensions, for which flow velocity or flow rate maximizes. The results from figure 5.8, suggest that this is true, since the velocities and flow rates increase from a geometry without the columns to a geometry including the columns. But, since the decrease in flow velocities due to the addition of the riser and downcomer columns is small, no major conclusions are drawn.

6.9. Horizontally stacked geometry

Horizontally stacked geometry was an attempt to simulate a more complex network where four modules are stacked on the same level next to each other. Observing the predicted values for flow velocity in

figure 5.9, no certain conclusions are drawn.

7

Suggestions for further improvement

By the end of the project, the model provides a better perspective of the behaviour of an electrolyser, with a flow driven by natural convection. The predictions, though, could be further improved.

As it was mentioned, experiments were not made possible, for the validation process, the results were compared to data from literature. In the reference articles, similar cases were studied but with a few differences. Consequently, experiments with the geometry used for the model can improve the validity of the model and show any other weakness. In addition, tuning of the parameters like friction factors and liquid properties can bring results similar to the two validation cases.

Moreover, an even distribution of bubbles was assumed in the electrode gap. In reality, a layer with high gas fraction is created close to the electrodes. This layer of gas bubbles and electrolyte mixture is called a plume. The thickness of the plume increases, across the electrode surface, in the direction of the flow. As a result, the thickest part of the plume is on the top of the electrode and the narrower is on the bottom. This uneven distribution of gas bubbles creates a flow velocity profile in the horizontal direction. It can even create a backflow in the electrode gap. Therefore, the model can be improved by including the effect of plume and velocity profiles. This means that, the model will become 2-dimensional or a correction factor can be introduced, to maintain the 1D nature of the model. This correction factor, may have an effect on the pressure drop to accommodate the distribution of gas bubbles in the electrode gap.

The bubble plume that is created, also affects the conductivity of the electrolyte liquid. As the gas fraction is increasing, the resistance is increasing. Consequently, current density is also uneven on the electrode surface and it should be modelled taking into account the gas fraction profile.

For a 2-dimensional model, a simulation with FEA software packages could improve the results. A more complex model, or geometry, could be solved with a FEA package to improve the resolution of the grid. As a result, a more detailed geometry can be assumed and the pressure drop can be calculated more accurately.

Further analytical analysis, may be beneficial because more effects of physical phenomena can be included, for example the effect of inertia and the kinetics of the electrochemical reaction, or a more general model can be developed with fewer assumptions.

Bibliography

[1] European Commission, *Renewable energy targets*, 2018. [Online]. Available: https://energy.ec.europa.eu/topics/renewable-energy/renewable-energy-directive-targets-and-rules/renewable-energy-targets_en.

[2] International Energy Agency, "Energy Technology Perspectives 2020," Tech. Rep., Feb. 2021. [Online]. Available: https://www.iea.org/reports/energy-technology-perspectives-2020.

[3] *Hydrogen Data*. [Online]. Available: https://hyjack.tech/hydrogen-data.

[4] Office of Energy Efficiency and Renewable Energy, *Hydrogen Storage*. [Online]. Available: https://www.energy.gov/eere/fuelcells/hydrogen-storage.

[5] F. Khatib, T. Wilberforce, O. Ijaodola, *et al.*, "Material degradation of components in polymer electrolyte membrane (PEM) electrolytic cell and mitigation mechanisms: A review," *Renewable and Sustainable Energy Reviews*, vol. 111, pp. 1–14, 2019. DOI: 10.1016/j.rser.2019.05.007.

[6] R. Phillips and C. W. Dunnill, "Zero gap alkaline electrolysis cell design for renewable energy storage as hydrogen gas," *RSC Advances*, vol. 6, pp. 100 643–100 651, 102 2016, ISSN: 2046-2069. DOI: 10.1039/C6RA22242K.

[7] H. I. Lee, H. S. Cho, M. J. Kim, *et al.*, "The structural effect of electrode mesh on hydrogen evolution reaction performance for alkaline water electrolysis," *Frontiers in Chemistry*, vol. 9, Nov. 2021, ISSN: 22962646. DOI: 10.3389/fchem.2021.787787.

[8] J. Haverkort and H. Rajaei, "Voltage losses in zero-gap alkaline water electrolysis," *Journal of Power Sources*, vol. 497, p. 229 864, 2021.

[9] S. . Petrovic, *Electrochemistry crash course for engineers*, 1st ed. 2021. Springer, 2020. DOI: 10.1007/978-3-030-61562-8. (visited on 08/23/2022).

[10] E. Amores, M. Sánchez, N. Rojas, and M. Sánchez-Molina, "Renewable hydrogen production by water electrolysis," *Sustainable Fuel Technologies Handbook*, pp. 271–313, 2021. DOI: 10.1016/b978-0-12-822989-7.00010-x.

[11] C. W. M. P. Sillen, E. Barendrecht, L. J. J. Janssen, and S. J. D. van Stralen, "Gas bubble behaviour during water electrolysis," *Hydrogen as an Energy Vector*, pp. 328–348, 1980. DOI: 10.1007/978-94-009-9042-5_30.

[12] H.-K. Park, J.-W. Han, and B.-J. Chung, "Influence of hydrodynamic parameters on the critical current density at water electrolysis: Mass flux, channel inclination and inlet void fraction," *International Journal of Hydrogen Energy*, vol. 47, pp. 7535–7546, 12 Feb. 2022, ISSN: 03603199. DOI: 10.1016/j.ijhydene.2021.12.138.

[13] J. Caire, G. Espinasse, F. Nicolas, and M. Peyrard, "Hydrodynamics of a fluorine electrolyser," in *Fluids Engineering Division Summer Meeting*, vol. 47519, 2006, pp. 457–462.

[14] M. Chisti, B. Halard, and M. Moo-Young, "Liquid circulation in airlift reactors," *Chemical Engineering Science*, vol. 43, no. 3, pp. 451–457, 1988.

[15] M. Schleiff, W. Thiele, and H. Matschiner, "Modeling and technical use of gas evolving electrodes. part 2: Modeling of gas-evolving electrolyzers with free electrolyte circulation," Tech. Rep., 1983.

[16] H. Vogt, "Instability of the two-phase flow in vertical interelectrode gaps," *Journal of applied electrochemistry*, vol. 29, no. 10, pp. 1155–1159, 1999.

[17] M. Caspersen and J. B. Kirkegaard, "Modelling electrolyte conductivity in a water electrolyzer cell," *International journal of hydrogen energy*, vol. 37, no. 9, pp. 7436–7441, 2012.

[18] P. Mandin, J. Hamburger, S. Bessou, and G. Picard, "Modelling and calculation of the current density distribution evolution at vertical gas-evolving electrodes," *Electrochimica Acta*, vol. 51, no. 6, pp. 1140–1156, 2005.

[19] Weisstein. “"hexagonal close packing" from mathworld.” (), [Online]. Available: https://mathworld.wolfram.com/HexagonalClosePacking.html (visited on 08/24/2022).

[20] I M. Krieger, “Rheology of monodisperse latices,” *Advances in Colloid and Interface Science*, vol. 3, no. 2, pp. 111–136, 1972. DOI: 10.1016/0001-8686(72)80001-0.

[21] R. Jamshidi, P. Angeli, and L. Mazzei, “On the closure problem of the effective stress in the eulerian-eulerian and mixture modeling approaches for the simulation of liquid-particle suspensions,” *Physics of Fluids*, vol. 31, no. 1, p. 013 302, 2019. DOI: 10.1063/1.5081677.

[22] J. W. Haverkort, “Natural recirculation electrolysis,” Private, ongoing work. (visited on 09/24/2022).

[23] F. Hine and K. Murakami, “Bubble effects on the solution ir drop in a vertical electrolyzer under free and forced convection,” *Journal of the Electrochemical Society*, vol. 127, no. 2, p. 292, 1980.

[24] I. Rousar, “Pumping effect due to gas evolution in flow-through electrolysers,” 1987, pp. 134–146.

[25] M. Carmo, D. L. Fritz, J. Mergel, and D. Stolten, “A comprehensive review on pem water electrolysis,” *International Journal of Hydrogen Energy*, vol. 38, pp. 4901–4934, 12 Apr. 2013, ISSN: 03603199. DOI: 10.1016/j.ijhydene.2013.01.151.

[26] Y. Luo, Y. Shi, and N. Cai, “Bridging a bi-directional connection between electricity and fuels in hybrid multienergy systems,” *Hybrid Systems and Multi-energy Networks for the Future Energy Internet*, pp. 41–84, 2021. DOI: 10.1016/b978-0-12-819184-2.00003-1.

[27] U. Luo and N. Cai, “Alkaline electrolysis,” *Encyclopedia of Electrochemical Power Sources*, 2009.

[28] D. W. Green, R. H. Perry, D. W. Green, and Knovel (Firm), *Perry's Chemical Engineers' Handbook, Eighth Edition*. New York, United States: McGraw-Hill Education, 2008.

A

Modelling and Navier-Stokes equations

The governing equation that describes the flow is the conservation of momentum paired with the conservation of mass. In three dimensions, the momentum equation has three Cartesian components. The z component, it is given by [28] with equation (A.1). It is a differential equation for the conservation of momentum, and it classifies as a Cauchy momentum equation. The current form is for an incompressible Newtonian fluid, and it is known as the Navier-Stokes equation.

$$\rho\left(\frac{\partial v_z}{\partial t}+v_x\frac{\partial v_z}{\partial x}+v_y\frac{\partial v_z}{\partial y}+v_z\frac{\partial v_z}{\partial z}\right)=-\frac{\partial p}{\partial z}+\mu\left(\frac{\partial^2 v_z}{\partial x^2}+\frac{\partial^2 v_z}{\partial y^2}+\frac{\partial^2 v_z}{\partial z^2}\right)+\rho g_z \tag{A.1}$$

where on the left side is the inertial term and on the right side, from left to right, are the pressure, viscous and gravity terms.

Alongside the momentum equation, the general mass balance, also known as the continuity equation, is written in the integral form, as it is found in [28]:

$$\frac{d}{dt}\int_{V_\alpha}\rho dV+\int_{A_\alpha}\rho\mathbf{w}\cdot\mathbf{n}dA=0 \tag{A.2}$$

where V_α is the arbitrary differential volume which is bounded by a surface of area A_α with $\mathbf{n}$ the outward unit normal vector A_α is the surface area of the arbitrary volume and $\mathbf{w}$ is the velocity of the fluid.